

FACILITY FORM 802

N65-22657
(ACCESSION NUMBER)

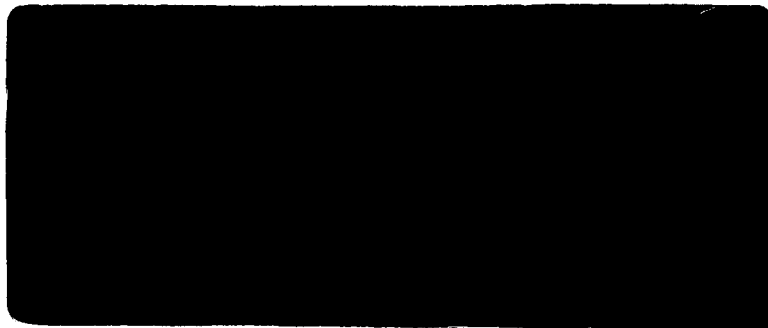
40
(PAGES)

CR-62446
(NADA CR OR TMX OR AD NUMBER)

(THRU)

1
(CODE)

03
(CATEGORY)



GPO PRICE \$ _____

OTS PRICE(S) \$ _____

Hard copy (HC) \$2.00

Microfiche (MF) .50



YARDNEY INTERNATIONAL CORPORATION

Investigation and Improvement of
Zinc Electrodes for Electrochemical Cells

Quarterly Report No. 2
October to December, 1964
Contract No. NAS-5-3873

National Aeronautics and Space Administration
Goddard Flight Center
Greenbelt, Maryland

Yardney Electric Corporation
New York, New York

Prepared by:


Z.O.J. Stachurski

Dr. G.A. Dalin

Approved by:



Frank Solomon, AVP

TABLE OF CONTENTS

	<u>Page</u>
1. Introduction	1
2. Results and Discussion	1
2.1 Zinc Penetration of Separators in a Cycled Silver-Zinc Cell.	1
2.2 Microscopic Investigation of Morphology and Growth of Zinc Deposits.	2
2.3 Kinetic Study of Zinc Deposition	3
2.4 Adsorption of Surfactants on Mercury Dropping Electrode.	7
2.5 Adsorption of Zincates in Separators.	9
3. Summary and Conclusions.	11
4. Program for Next Quarter.	13

1. INTRODUCTION

The previous report described the conditions under which various types of zinc deposits are formed. Four types of deposits were formed, 1) smooth 2) foam 3) dendritic and 4) heavy sponge, with the form dependent on the plating overvoltage.

Heavy sponge was considered the late stage of dendritic deposit under conditions of restricted growth. This last form appears to be responsible for penetration. It was found that penetration through the cellophane separators took place by growth of heavy sponge into the separator rather than by mechanical piercing of the membrane.

The work of the second quarter was designed to supply quantitative data on the rate of growth under carefully controlled conditions to determine the effect of the nature of the separator on the growth mechanism and to determine whether surfactants can affect the nature of the growth. In order to tie this more fundamental work to phenomena noted in actual cells, our presentation will start with a description of the growth through the separators of a cycled cell.

2. RESULTS AND DISCUSSION

2.1 Zinc Penetration Of Separators In A Cycled Silver-Zinc Cell

Separators were removed from cells which had been cycled until failure by zinc penetration occurred. The C-19 separators were sealed in plastic, polished up to a penetrated spot, and microphotographs were taken. Four layers of C-19 can be seen in Fig. 1 (200x). The picture shows a section through a penetrated place. The horizontal arrows indicate the outside layers. The inside layers of C-19 are lighter.

Zinc penetrated the first layer and expanded in the vertical plane. It is visible that the penetrating deposit is spongy. No dendritic type of deposit appears. Spongy nodules as large as the one shown here were seen compressing the next layers of separators by about 50% without causing a break in the C-19. Fig. 2 shows how the sponge expands after penetrating the first layer. It fills the free space between the separators and pushes them apart. Fig. 3 shows a spot in which sponge penetrated all of the layers except for the last. Disintegration of the separators is much more advanced than in Fig. 1 and sponge pervades the entire region.

Expansion of sponge after penetration of a second layer of separator is shown in Fig. 4. Arrows point to the first and last layers of C-19. The above set of pictures confirms the opinion given in report No. 1 that it is a heavy sponge type of deposit which is responsible for zinc penetration of separators. No sharp crystalline dendrites piercing the cellophane film were found.

2.2 Microscopic Investigation of Morphology and Growth of Zinc Deposits

Zinc deposits were grown in a microcell which was described in report No. 1. The cell had 3 zinc electrodes: test, counter and reference. The test electrode was wrapped in one of three types of separators: 0.0010" cellophane, DuPont PUD0-300; 0.0015" Polyvinyl Alcohol (PVA), and 0.0011" Grafted Polyethylene*. The purpose of the experiments was to find differences in morphology of zinc penetration among chemically different membranes. Zinc plating was carried out galvanostatically. All separators were pre-soaked 14 hours before plating. Figures 5 through 7 show penetration of a cellophane separator. Penetration through PVA is shown in Fig. 8 and Fig. 9. No ZnO was added to the 31% KOH used as an electrolyte. Only a small quantity of zincate was formed by corrosion during wet stand. This was to impose the most favorable conditions for formation of dendrites. In Fig. 5 we see (from the left) the zinc electrode (sides protected by epoxy coating), space filled by the electrolyte and a membrane. Immediately after starting the current (30mA/in²) the zinc overvoltage (η) is only -4mV. It rises to -310mV in 90 minutes. After that time the inception of penetration is visible as a number of nodules growing into the separator (Fig. 6). One of them penetrates first, the overvoltage drops (Fig. 7) and the penetration in other places slows down; zinc deposited before the moment of penetration belongs to a heavy sponge type. After penetration it becomes dendritic (Fig. 7).

Penetration of zinc through PVA (Fig. 8) has basically the same character as through cellophane but there are differences. Zinc does not grow into the PVA on a wide front. Nodules of zinc in PVA are narrower than in cellophane. Completed penetration is shown in Fig. 9.

It was important to know if surfactants change the character of the deposits. A solution saturated with Igepal CO-730 (General Aniline and Film) was used in the microcell. All other conditions were maintained as in the experiments shown in Fig. 5 through Fig. 10. Cathodes were wrapped in grafted polyethylene (Fig. 10 and Fig. 11) and in PVA separators (Fig. 12).

It was found that the type of deposit was changed from heavy sponge type to dendritic by the surfactant. Penetration did not occur during the same period in which PVA was penetrated without the Igepal, but statistical data are not as yet available.

In another experiment, zinc cathodes wrapped in PVA and in cellophane as a control were plated overnight in microcells in 30% KOH saturated with zincate. Separators were penetrated and the results are shown in Figs. 13 through 16. The separators were taken out of the cells and examined. Deposits grown in the separators are hexagonal crystalline dendrites. There is no

*Radiation Applications Inc., 40/100 Grafted Polyethylene 0.0011" thick.

essential difference between the deposits in PVA and cellophane. The diameter of dendrites in PVA is 2 to 3 times greater than in cellophane.

Penetrated grafted polyethylene is shown in Fig. 17 and 18. The deposit is crystalline, but the diameters of the dendrites are much smaller than in cellophane under similar conditions. In general the mechanism of growth of Zn in the various separators tested seems to be the same.

The influence of various separators on the morphology of zinc deposits seemsto be primarily due to differences in the rate of diffusion . Such differences are indicated in Fig. 19. The curves show the changes in zinc overvoltage in 3 microcells connected in series. Cathodes in these cells were wrapped in cellophane, grafted polyethylene and PVA. The cells stood wet for two hours before turning on the current ($30\text{mA}/\text{cm}^2$). The overpotential initially rises due to decrease in concentration of zincates present in the space between the cathode and the separators. The curves have a maximum after which stationary conditions of plating are established. The resistance overpotential can be responsible only for a small part of the total. The major differences are due to differences in diffusion of zincates through the separators. The fastest diffusion of zincate is therefore through a cellophane separator. The above test gives only qualitative information. Values of diffusion coefficients will be given in the next report.

2.3 Kinetic Study of Zinc Deposition.

Among the parameters characteristic for the whisker type of metal deposition the most important is the rate at which the whiskers grow. In the case of a foam or a sponge it is difficult to arrange to study the growth of a single whisker. However, we can measure the mean of the rate of growth of many whiskers in a given direction; this is apparent as the movement of the front of the deposit.

A special cell, which we have termed a tunnel cell, was built for measuring the rate of growth of zinc deposits. The cell is shown in Fig. 20. The tunnel (2) consists of a series of 8 plexiglass shims through which is drilled a central hole with a cross sectional area of 0.635cm^2 . The length of the tunnel, is $5/8"$. Sixteen silver contacts (3) are located between the shims, and the 8 shims are cemented together.

The block is cemented to a similarly drilled cell case. A zinc sheet (1) to serve as cathode is cemented to the outer face of the block. The seventeenth contact is attached to the zinc cathode for the double function of measuring the current and disclosing the extent of zinc growth.

In order to measure the extent of zinc growth, the contacts are wired to the multi-point switch (4) and the meter (5) to show the difference in potential between each successive contact and the cathode. As the zinc deposit (8) reaches each contact, it shorts it out reducing the potential difference to zero. From the chart, it is thus possible to follow the rate of zinc growth.

Zinc sheet is used as the counter electrode (7). Constant potential against the zinc reference electrode (6) is maintained by a potentiostat (9). Current is measured periodically by means of a very low value dropping resistor which introduces a negligible error in the potential.

The thickness of the deposit as a function of time for various potentials is shown in Fig. 21. Deposition of zinc was conducted from 44% KOH containing zincate (40% of saturation). At -42mV zinc overpotential (curve 1) the thickness of the deposit does not increase linearly with time but rather accelerates, also the current of deposition increases with time (curve 1a). At slightly higher overpotential, -61mV, the length of zinc whiskers increases much more rapidly (curve 2) and the dependence is more linear with time. Here also, the current rises (curve 2a). In both cases foamy soft deposits were obtained. At still higher overvoltage, -144mV, the zinc deposit grows linearly with time but much more slowly than at -61mV (curve 3). The current during the experiment (curve 3a) is almost constant. It should be mentioned here that after every plating the deposits were examined microscopically.

Special emphasis was put on the parts of the deposits corresponding to the beginning and the end of the plating. Returning to curves 3 and 3a of Fig. 21 - the corresponding deposits were mixed - dendrites and foam. At the beginning of the plating more foam was present while at the end, more dendrites. It is clear therefore that at zinc overpotentials somewhere between -61mV and -144mV and for the given solution, a critical potential exists at which the deposit changes from a foam formed of very fine whiskers to dendritic.

We can draw another important conclusion: the passage from whiskers to dendrites is not continuous. There is no intermediate form. No whiskers of intermediate size were found. Comparing current corresponding to the above deposits, we find that during the first hours of plating (below 10 hours) - the higher the overvoltage the higher the plating current; however, with time the difference decreases and between 10 and 30 hours the relation is completely reversed. This we can explain only if we assume that the real plating area is much higher at low overpotentials and lower at higher overpotentials after a sufficiently long time of plating.

Consider now plating at two different concentrations of zincate at high overpotential (-144mV). The data are shown in Fig. 22. Curve (1) for 40% saturated zincate in 44% KOH represents the

dependence of thickness of the zinc deposit on time while (2a) represents the corresponding current. The concentration of zincate is approximately constant during the plating operation because a zinc anode was used. Deposition and dissolution of zinc are therefore balanced and the initial bulk concentration of zincate remains essentially uncharged. Only a slight disturbance of the balance could be caused by zinc corrosion or hydrogen evolution on the cathode. Let us now compare curves (1) and (1a) with (2) and (2a). The latter were obtained at one-half the zincate concentration of the former. The thickness of the deposited zinc layer increased linearly with time in both cases. The rate of growth was higher at higher concentration, but there is no direct proportionality between the rate of growth and concentration. The same is true of the currents. The current in the more concentrated solution of zincate is roughly as much higher as is the rate of growth. The deposit in KOH at 40% of zincate saturation solution was a mixture of foam and dendrites. In a solution at 20% of saturation only foam was found both at the beginning and at the end of plating. This was contrary to expectation. It was expected that dendrites would form more readily in the more dilute zincates. It is possible that some optimal condition exists for transition from foam to the dendrites.

It was previously stated that some surfactants as for example Igepal influence the morphology of the zinc deposits. In Fig. 23 it is shown how Igepal influences the rate of growth of zinc and the plating current at constant potential. The thickness of the deposit without Igepal (curve 1) increased more rapidly than in the presence of saturated Igepal (curve 2). The solubility in 44% KOH is less than 0.02%. The plating current was higher with Igepal (curve 2a) than without (curve 2a). The effect was definite despite the fact that only two points were available for comparison.

Even more interesting than the comparison of changes in thickness (x) of the deposits is comparison of velocities of growth (dx/dt) as a function of time (Fig. 24), or of distance from the zinc electrode (Fig. 25). Let us first compare velocities of growth after the same time, for example after 8 hours (Fig. 24). Consider rates at various potentials, but in the same solution (44% KOH, 40% saturated ZnO). At -42mV (curve 4) plating proceeded at approximately constant rate of whisker growth for about 2 hours at 6.7×10^{-6} cm/sec, then started to accelerate reaching 3×10^{-5} cm/sec, after 12 hours. This rate was the highest obtained in our experiments. The deposit was foamy. At -61mV steady plating proceeded at 2.7×10^{-5} cm/sec. (curve 3). At -114mV (curve 1a) the rate of growth decreased to 6.7×10^{-6} cm/sec. Therefore after a sufficiently long time we have an increase of rate of growth with increase of overpotential.

Rates of growth of the zinc whiskers with and without a surfactant for 80% saturated zincate at -50mV are given in curves 2a and 2. The rate in the presence of Igepal is lower. Both are constant. At -114mV at two different concentrations of zincates the rates

are constant, that at higher concentration being higher but not in direct proportion to the concentration. A similar picture is obtained when rates are compared at various distances from the basic electrode, (Fig. 25).

It was known that zinc deposits from zincate solutions have low density, but it was interesting how this density changes with changes in the plating conditions.

The tunnel cell also supplied information as to the change in density of the deposit with time. In this cell plating takes place in one direction, (x) and the volume is proportional to x. The rate of zinc growth, dx/dt , was measured. The current density at any moment is known. This permits us to calculate the quantity of zinc plated during the time, t. This is based on the assumption that hydrogen evolution is negligible at low zinc overpotentials in solutions containing zincates.

Assume that with a small mass of plated zinc, dm , is associated a small increase in the volume of zinc, dV . Hence we can write an expression for the instantaneous density ρ_t :

$$\rho_t = \left(\frac{dm}{dV} \right)_t = \frac{i \cdot s \cdot e \cdot dt}{F \cdot s \cdot dx} = i \frac{e}{F} \left(\frac{1}{dx/dt} \right)_t$$

Where: s- area of a crosssection of the tunnel cell; F- Faraday's number and E- equivalent weight of zinc.

The dependence of density on time at various zinc overpotentials is shown in Fig. 26. In a solution of 44% KOH containing zincate (40% of saturation) the density of the deposit varies considerably with time but the variation with zinc overpotential is even more pronounced. Curve 1 of Figure 26 represents the variation of density with time of a zinc deposit obtained at -42mV zinc overpotential. The porosity of this foam is 99.8%. At the slightly higher overpotential of -61mV foam was also obtained. The thickness of the whiskers in the foam is almost constant at about $0.8\mu \pm 0.3\mu$ for -42 and -61mV overpotentials. At -111mV a sudden jump in the density to 0.18g/cm^3 (curve 3) occurs. Microphotography shows that the deposit is dendritic although some foam is admixed. The diameters of the dendrites were 25-50 μ . Figure 27 shows how strongly the density varies with overpotential.

Densities of the deposits obtained at high overpotential (-111mV) in KOH solutions at 20% of zincate saturation are shown in Fig. 28 (curve 2) and are compared with the density of the deposit obtained from a solution containing 40% saturated zincate. There is no great difference between the curves.

Plating from a solution saturated with the surfactant - Igepal led to a deposit which was much denser (Fig. 29, curve 2) than without the surfactant (curve 1). It was previously mentioned that Igepal

has a strong effect on the morphology of the deposition. It is obvious therefore that Igepal has a definite influence on the kinetics of electrodeposition of zinc. In order to investigate the effect of surfactants on kinetics, the adsorption of a number of surfactants was studied using A.C. Polarography.

2.4 Adsorption of Surfactants on a Dropping Mercury Electrode.

It is known that some but not all surfactants influence zinc penetration through separators and therefore the mechanism of zinc electrodeposition. To influence the mechanism, a surfactant must be adsorbed at the surface of the deposited metal. The assumption of adsorption is necessary because usually the concentration of surfactants present in electrolyte is low. Surfactants adsorbed at the interface, between the electrode and the electrolyte, decrease the electrical double-layer capacity. This decrease is an approximately linear function of the surface excess of the surfactant. Most metals adsorb organic substances up to a similar potential which is negative relative to the electrocapillary zero. It seems therefore reasonable to study the adsorption of surfactants on the mercury electrode and to transfer the conclusions back to zinc. As a method of determining double layer changes the Breyer-Guttman A.C. method was utilized. In this method a test electrode of the dropping mercury type is continuously polarized negatively while a small A.C. component of constant voltage amplitude (30mV) was applied. A "Metrohm" polarograph with an A.C. unit was used for the study. The A.C. current was recorded vs. D.C. potential, after separation from D.C. by a capacitor.

This method is less accurate than Grahame's bridge method, but is accurate enough for the purpose. The discrepancy is mainly in the region of large A.C. current due to IR drop. Breyer's method measures differential pseudo capacity as well as real D.L. capacity. The reversible current of zinc ion reduction is recorded in this method as a peak.

To standardize the A.C. polarogram in units of differential double layer capacity ($\mu\text{F}/\text{cm}^2$) it was taken into account that at potentials higher than one volt vs. Hg/HgO the double layer capacity is entirely determined by the cation of the electrolyte and the influence of the anion is negligible. For the standardization of our A.C. polarogram we used the value of $16.1 \mu\text{F}/\text{cm}^2$ at -1.16V vs. calomel electrode in 0.1N KCl given by D.C. Grahame.

An A.C. polarogram obtained in 0.1N KOH calibrated according to the above value is shown in Fig. 30 curve 1. Curve 2 represents the dependence of double layer on the potential as given by Grahame.

Although for battery purposes the adsorption of surfactants at high electrolyte concentrations is more significant, it was investigated in 0.1N KOH first. We did so because the influence of surfactants on D.L. capacity is better known in dilute solutions. Later on we investigated also surfactants in concentrated solutions (31% KOH).

It is known that surfactants adsorb at the metal - electrolyte interface only in certain ranges of potentials around the potential of zero charge. At potentials higher than certain specific desorption potentials which are different for various organic compounds the surfactants cannot exist at the surface in the adsorbed state. Desorption is marked by a sudden change in surface charge reflected by a peak on the D.L. vs. potential curve. The potential at which this peak occurs is called the desorption potential.

Consider now Fig. 31. It presents the influence of two surfactants - Igepal CO-730 (polyphenoxypoly (ethyleneoxy) ethanol) curve 3) and Triton X-100 (curve 4) on the double layer capacity on mercury. Curve 1 is the supporting electrolyte, 0.1N KOH, without the surfactants. Curve 2 is obtained in the same electrolyte but in the presence of $10^{-3}M$ ZnO. Both surfactants are strongly adsorbed at potentials up to -1600mV as is shown by the much lower value for the double layer capacity. At -1600mV, a sudden desorption peak occurs. The desorption potentials are here much more negative than the reversible potential of zinc in this solution. The pseudo capacity peak of zinc is shown in curve 2 and the very beginning of it indicated approximately the reversible potential of zinc. We can transfer now the conclusion from the mercury electrode to the zinc electrode and state that in dilute KOH solutions we can expect the adsorption of both surfactants tested on zinc at its reversible potential and up to -0.5V overpotentials.

The same conclusion can be drawn with respect to the surfactants shown in Fig. 32. The compounds tested were 3M brand fluorocarbon surfactants. Curve 2 shows the A.C. polarogram of FC-19 anionic fluorocarbon surfactant which is characterized by excellent chemical stability.

Curve 3 is an A.C. polarogram of a solution containing FX-161, an anionic fluorocarbon. Curve 4 was obtained using a cationic fluorocarbon, FC-134. The adsorbability of the above surfactants is low and therefore no further work done with them. Cationic fluorocarbon gives an interesting maximum at a potential close to zero charge potential. It is probably related to rearrangement of the ionic surfactant at the surface when the negative charge increases.

The strongly surface active substances Triton X-100 and Igepal were tested also in 31% KOH. Because of low solubility in KOH,

saturated solutions were used. The results are shown in Fig. 33. Curve 1 was obtained in 31% KOH, Curve 2 was obtained in 31% KOH saturated with Triton X-100, Curve 3 was obtained in 31% KOH saturated with Igepal. Curve 4 was obtained in KOH containing $10^{-3}M$ zincate. It is apparent that sharp desorption of Triton starts at a potential more positive than the reversible potential of zinc. Consequently it follows Triton cannot influence the way in which zinc plates out of 31% KOH. Contrary to this, curve 3 shows that Igepal has no sharp desorption potential and its desorption extends up to $-300mV$ which is more negative than the reversible potential of zinc. In this case we can expect that up to an overpotential of $-300mV$ on zinc, Igepal will be adsorbed at the electrode and can influence the electrochemical deposition of zinc. This agrees with observations that Igepal influences the type of the deposit strongly while Triton does not. Also the time of penetration through membranes is influenced by Igepal and not by Triton.

In general, this experiment suggests the explanation why some surfactants have a marked influence on zinc plating and others do not. Moreover, it indicates that the procedure outlined constitutes a valuable screening test.

2.5 Absorption of Zincates in Separators

In sections 2.3 and 2.4 we discussed the problem of direct electro-deposition of zinc from free solution of zincate. We come now to the effect of the separator on the growth process. During the early stages of the deposition, the separator prevents growth in the direction normal to the surface. Eventually, as is well known, zinc whiskers or dendrites grow inside of the separator. It would seem that the rate of this growth should be dependent on the concentration of zincate in the separator.

Cellophane, PVA and grafted polyethylene separators were soaked for 5 days in 41% KOH containing zincate in amounts from $10^{-3}M/l$ to saturation. After this period they were removed from the solution, the surface was dried by toweling and they were weighed and then decomposed at $550^{\circ}C$ in a furnace. ZnO was extracted with a hot 1M ammonia buffer and centrifuged and polarograms were run with gelatin as maximum suppressor. Because the quantity of adsorbed liquid was known, the apparent concentration of zincates in the adsorbed liquid could be calculated. The results are shown in Fig. 34. The interrupted line in this figure shows approximately how the concentration of zincate would rise in the separator with increasing concentration of zincate in the solution surrounding the membrane, assuming the Nernst separation coefficient between two phases to be equal to one. The change in KOH density due to zincate is neglected. This straight line would be obtained if separators did not interact in any way with zincate and if the composition of the liquid entering the separator remained unchanged. Fig. 34 shows that this is not the case. Consider first low con-

concentrations of zincate, say up to 0.2Mole/liter. The apparent concentrations of zincate in the absorbed liquid are higher than the dotted line predicts. Zincate therefore is accumulated in the membrane at low concentrations. This takes place in all three types of membranes. The internal analytical concentration of zincate in the separators rises rapidly with concentration in the external zincate and reaches a plateau. The plateau on curves (1) and (2) for cellophane and PVA is below the saturation concentration. Therefore we have to exclude the possibility of precipitation of solid ZnO . Consequently, it appears that adsorption of zincate on both separators takes place.

It is possible that in the case of grafted polyethylene we have adsorption as well but there we cannot exclude the possibility of precipitation. Increase of external concentration from 0.4M/liter and to 1.0M/liter causes a much smaller increase in concentration inside the membrane. The concentration of zincate inside the membrane is lower in this range than in the external solution. Finally, at external concentrations above 1 mole/liter plateaus are reached. It is suggested that these plateaus are related to the saturation of the liquid inside of the separators with zincate. We can therefore separate the zincate adsorbed at the surface of micro-fibers of cellulose or PVA, and zincate in the electrolyte present between them. The third possible form of zinc in the separator is ZnO precipitated among the fibers.

Based on the above explanations, the relation between the zincate in the separator and the concentration of zincate in the external solution can be considered as an adsorption isotherm. Adsorption isotherms of zincates on various separators are given in Fig. 35. Adsorption is greatest on cellophane (1). Next is grafted polyethylene (3) and lowest is PVA.

The relative concentrations of zincate internal to and external to the separator must be involved in the mechanism of zinc penetration in accordance with the following argument. In the plating operation, zinc grows toward the richest source of zincate. This was shown clearly in several different ways. In a micro-cell zinc grows initially toward the separator. As the zincate is exhausted in this region, the dendrites proceed around the edge of the cathode toward the insulated back where the zincate concentration is still high. This takes place despite the fact that the counter-electrode is positioned in the opposite direction. On the other hand, if the separator is mechanically perforated prior to the experiment, growth after the initial period will proceed with great rapidity toward the opening through which zincate is diffusing.

The rate of growth of a specific dendrite or tendril is therefore dependent on the rate at which zincate reaches the tip of the spear. This rate, in turn depends on the concentration difference and the diffusion coefficient.

Now we can consider the case of a dendrite in contact with the surface of a separator. If the rate of diffusion of zincate to the dendrite is greater from within the separator than from without, then the dendrite will grow into the separator. This must obviously be the case when the external solution is exhausted of zincate by rapid deposition. So at sufficiently high current densities any separator must be penetrated. Conversely, at sufficiently low densities, replenishment of the external solution by diffusion through or from within the separator can occur and thus prevent penetration. Experience with actual cells confirms these views.

The critical current density below which penetration does not occur must then be a function of the relative internal and external concentrations and diffusion rates. The measurement of these quantities for a variety of separators will be a principal objective of the research in the next quarter.

3. SUMMARY AND CONCLUSIONS

It was established that in actual Ag-Zn cells as well as in micro-cells, zinc penetration occurs by the deposition of heavy sponge nodules within the separators. After passing through the separator (C-19) the growth expands between the separators as a sponge. Penetration takes place by growing into the separator and not by mechanical puncture. In actual cells as distinguished from micro-cells, dendritic growth within the separator does not occur because charging current densities are always low.

Experiments in micro-cells show that the underlying mechanism of penetration through cellophane, PVA and grafted polyethylene is basically similar. There are differences in morphology of the penetrating deposits. Zinc does not grow into PVA on a wide front as it does in cellophane. Nodules of zinc growing through are narrower in PVA, and even narrower in grafted polyethylene.

It was found that surfactant (Igepal CO-730) changed the morphology of the deposits from heavy sponge to typically dendritic. The form of the deposit was influenced simultaneously by the surfactant and the separator used. The separator influenced the deposit through control of the rate of diffusion of zincates.

The rate of growth of zinc deposits was studied potentiostatically in a special tunnel cell. The rates of growth (in cm/sec) were found to be nearly constant with time in most cases.

The rate of growth of the deposit decreases rapidly with increasing overpotential while the density of the deposit increases. At high overpotentials increase in density is associated with the dendritic type of deposition. At low overpotentials zinc is always deposited as a foam with whiskers of diameter 0.6 μ - 1.0 μ . At low overpotentials the diameters of the whiskers seem to be independent of conditions. During plating in free electrolyte no forms

intermediate between foam and dendrites were encountered. The passage from whiskers to dendrites seems to be very sharp. On the contrary in separators we find a continuous range of diameter of dendrites.

Adsorbability of surfactants was measured utilizing their ability to decrease the electrical double layer capacity. It was found that in dilute KOH all surfactants tested were adsorbed on mercury at the plating potentials of zinc. In concentrated KOH (31%) only Igepal was capable of adsorption. Subsequently, it was found that saturated Igepal causes a large difference in the density of the zinc deposits (2 to 3 times) and in dilute solutions of zincate changes the morphology of the deposits (heavy sponge to dendrites).

Separators soaked in 44% KOH containing varying concentrations of zincate were analyzed. A strong adsorption of zincate in the separators is indicated. The quantity of zincate per volume of absorbed electrolyte in cellophane and PVA is lower than the concentration of zincate in the surrounding solution at high zincate concentrations. In low zincate concentrations (e.g. 0.1M/liter) the separator contains more zincate per volume of liquid than the surrounding electrolyte. This provides a clue with respect to the conditions which give rise to penetration. When the zinc electrode is on charge, and a growth is in contact with the membrane and the concentration of zincate near the separator is depleted below that within the separator and the overpotential is rising, the deposit becomes denser and at the same time plating starts to move into the separator.

PROGRAM FOR THE NEXT QUARTER

- 1) Using the methods described in the 1st and 2nd report develop the conditions leading to the change from foam to sponge deposition.
- 2) Determine the diffusion coefficient of zincates in separators in the range of conditions corresponding to overcharge.
- 3) Study zinc overpotentials during the process of zinc shape change on cycling.
- 4) Same on overcharge.
- 5) Attempt to give a quantitative model of zinc penetration.

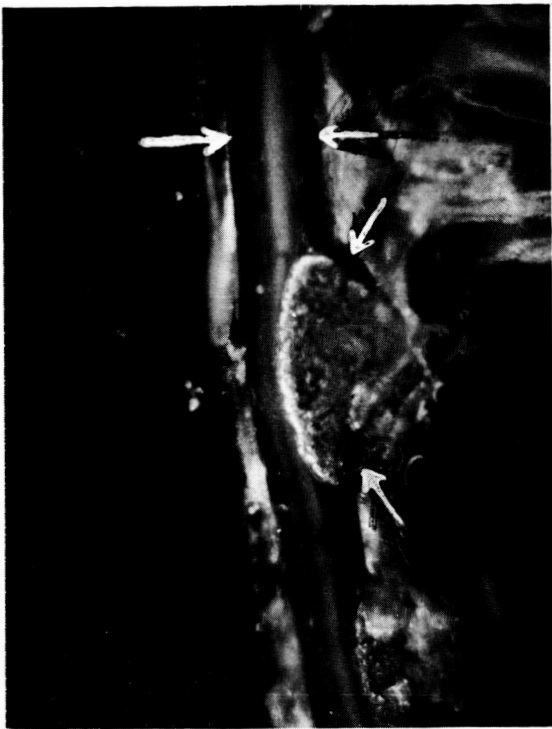


Fig. 1 200X



Fig . 2 200X

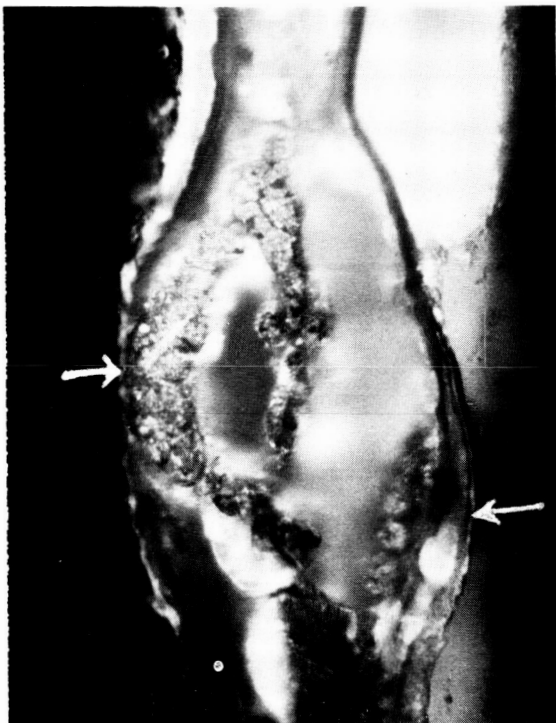


Fig. 3 200X



Fig. 4 200X

Three Stage Penetration Of Cellophane
31% KOH 30 mA/cm sq.

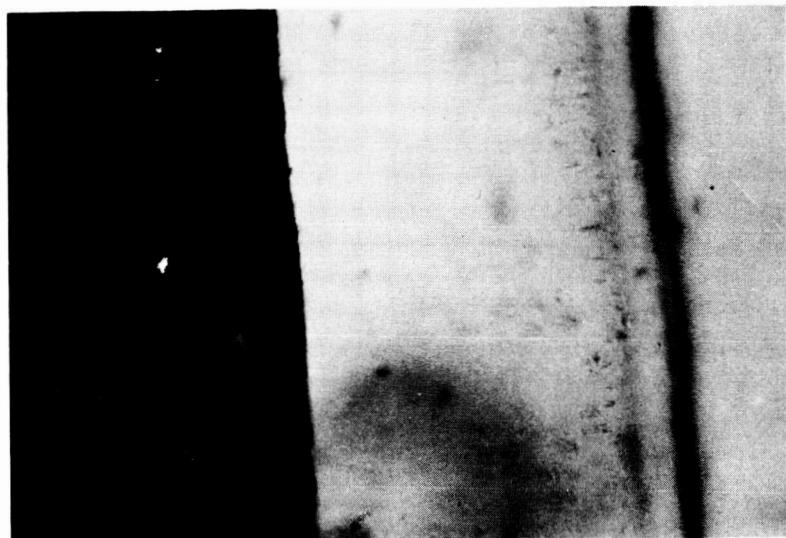


Fig. 5

$t = 0$

$\eta = -4 \text{ mV}$

$1\text{mm} = 10\mu$



Fig. 6

$t = 90 \text{ min.}$

$\eta = 310 \text{ mV}$



Fig. 7

$t = 135 \text{ min.}$

$\eta = 140 \text{ mV}$

Three Step Penetration Of PVA
31% KOH 30 mA/cm sq.



Fig. 8

$t = 195 \text{ min.}$

$\eta = 320 \text{ mV}$

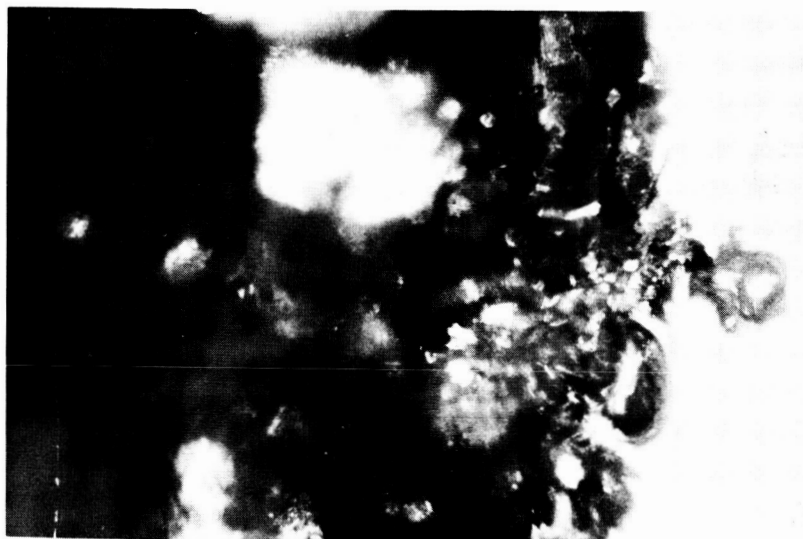


Fig. 9

$t = 200 \text{ min.}$

$\eta = 315 \text{ mV}$

Dendrites in Igepal
31% KOH 30mA/sq. cm.



Fig. 10
 $\eta = 137$ mV
 $t = 180$ min
100X

Grafted polyethylene

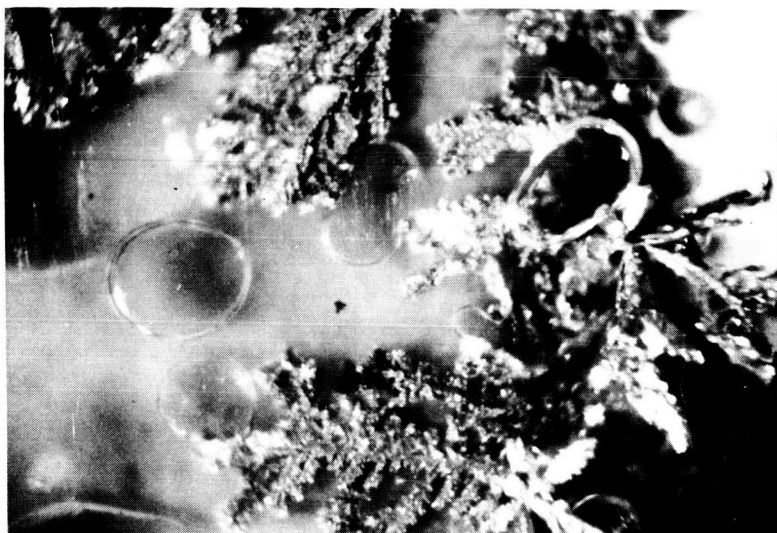


Fig. 11

$\eta = 135$ mV
 $t = 240$ min

Grafted polyethylene



Fig. 12

$\eta = 13$ mV
 $t = 240$ min

PVA

Penetrated PVA
30% KOH sat ZnO
30 mA/ sq. cm.

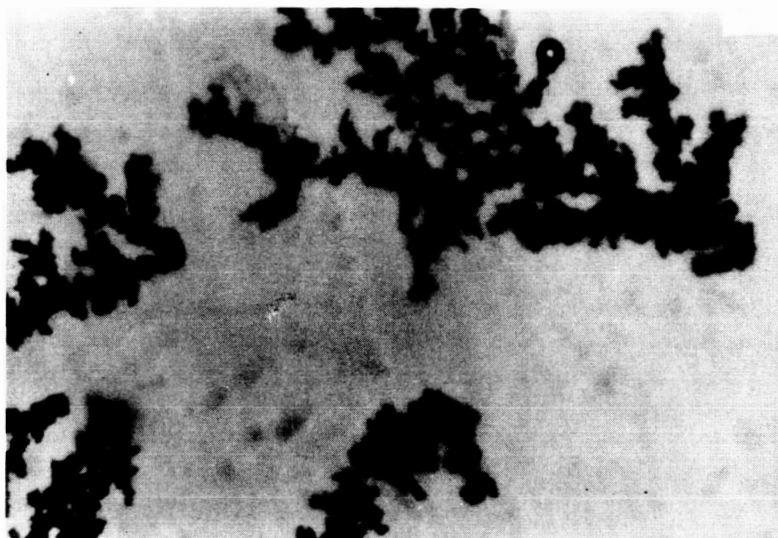


Fig. 13

100X

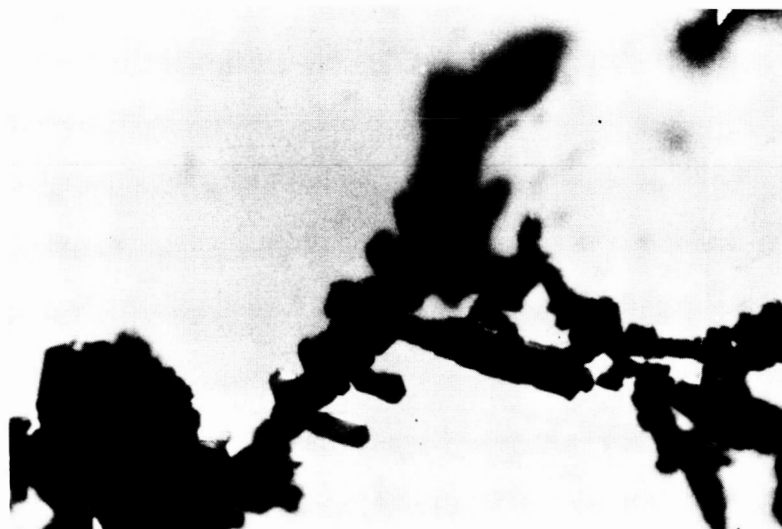


Fig. 14

400X

(one mm on the
picture = original
2.5 μ)

Penetrated Cellophane
30% KOH sat ZnO
30 mA/ sq. cm.

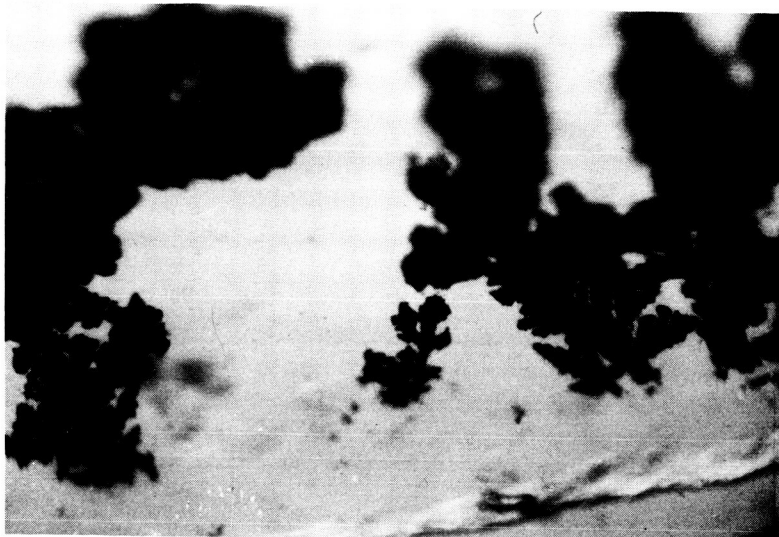


Fig. 15

400X

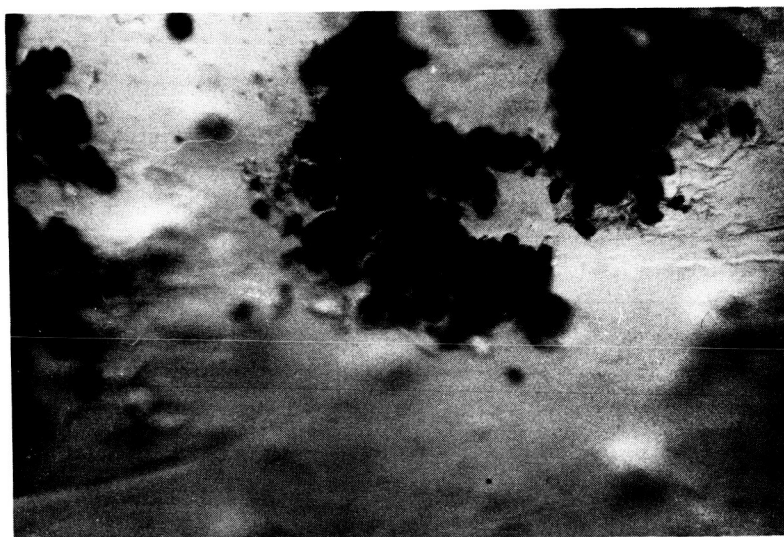


Fig 16

400X

Penetrated Grafted Polyethylene
44% KOH 80% ZnO

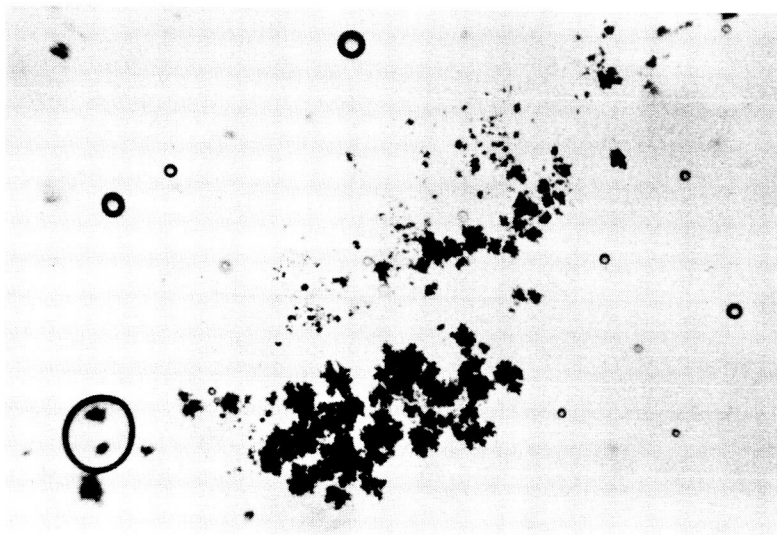


Fig. 17

100X

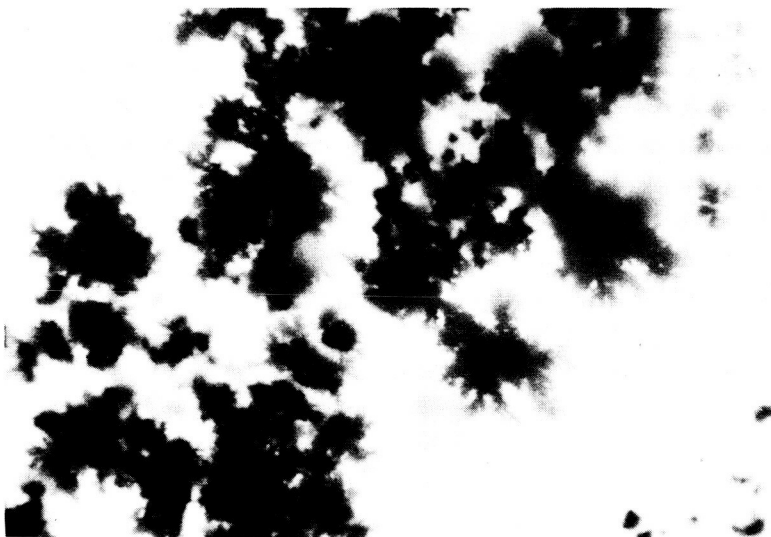


Fig. 18

400X

DEPENDENCE OF OVERPOTENTIAL ON TIME IN THE MICRO CELL.

30 mA/cm² 30% KOH, SAT. ZnO

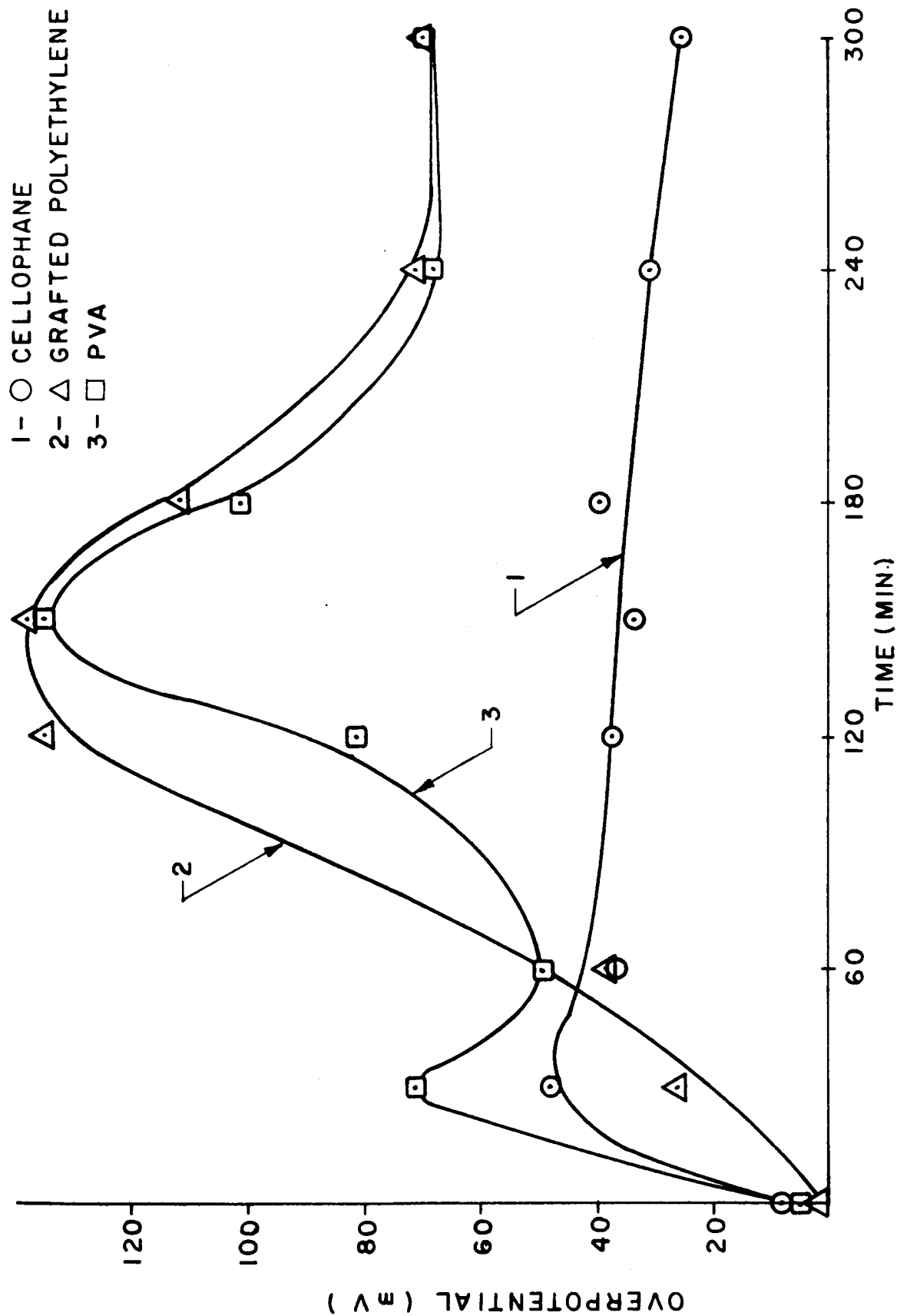


FIG. 19

TUNNEL CELL APPARATUS.

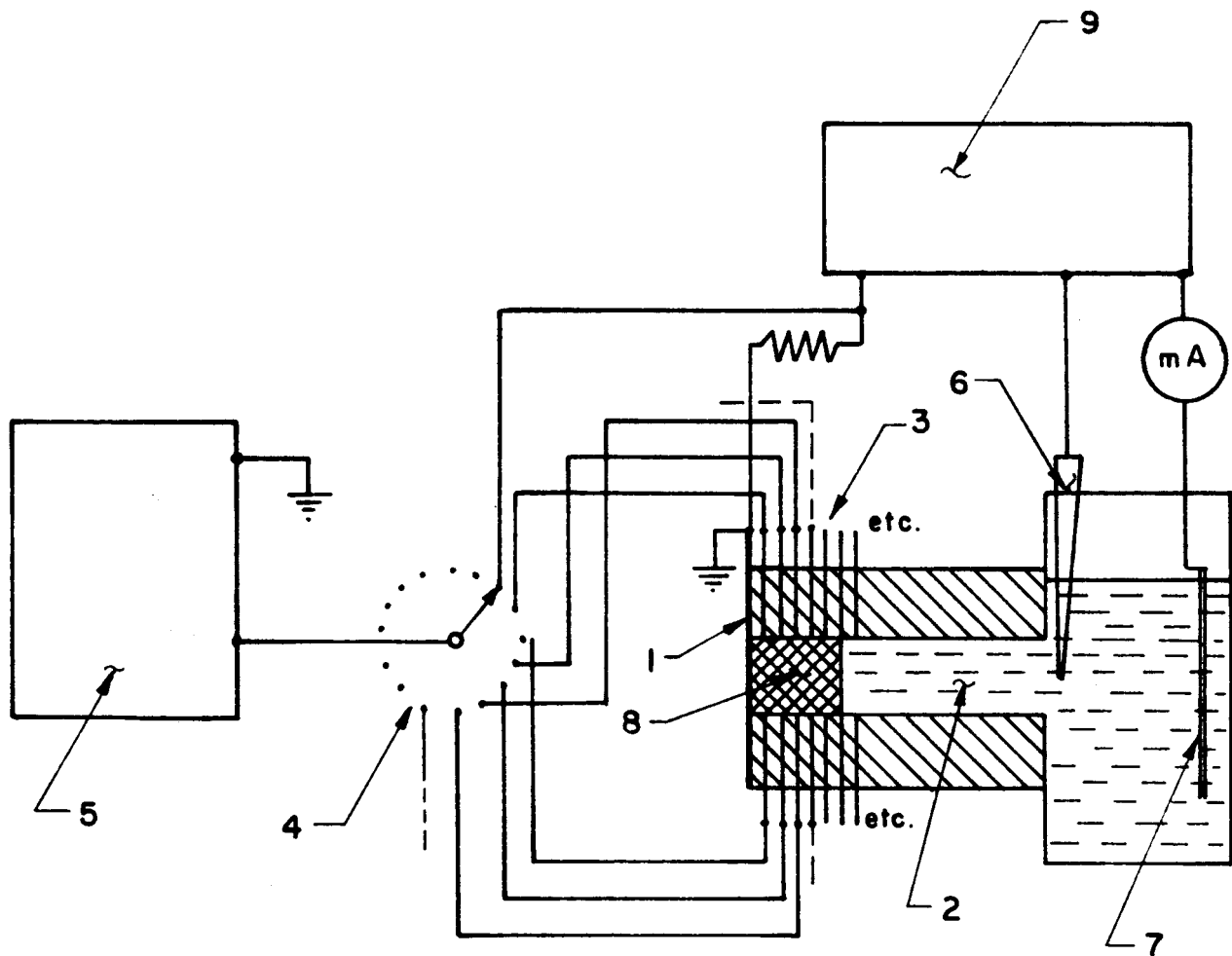


FIG. 20

DEPENDENCE OF THICKNESS OF THE DEPOSIT IN THE MICRO CELL ON TIME AT VARIOUS OVERPOTENTIALS.

- 1a- \triangle CURRENT DENSITY } 42 mV/44% KOH/40% SAT. ZnO
- 1- \triangle DISTANCE
- 2a- \square CURRENT DENSITY } 61 mV/44% KOH/40% SAT. ZnO
- 2- \square DISTANCE
- 3a- \circ CURRENT DENSITY } 144 mV/44% KOH/40% SAT. ZnO
- 3- \bullet DISTANCE

ZnO CONTENT GIVEN AS PER CENT OF SATURATION

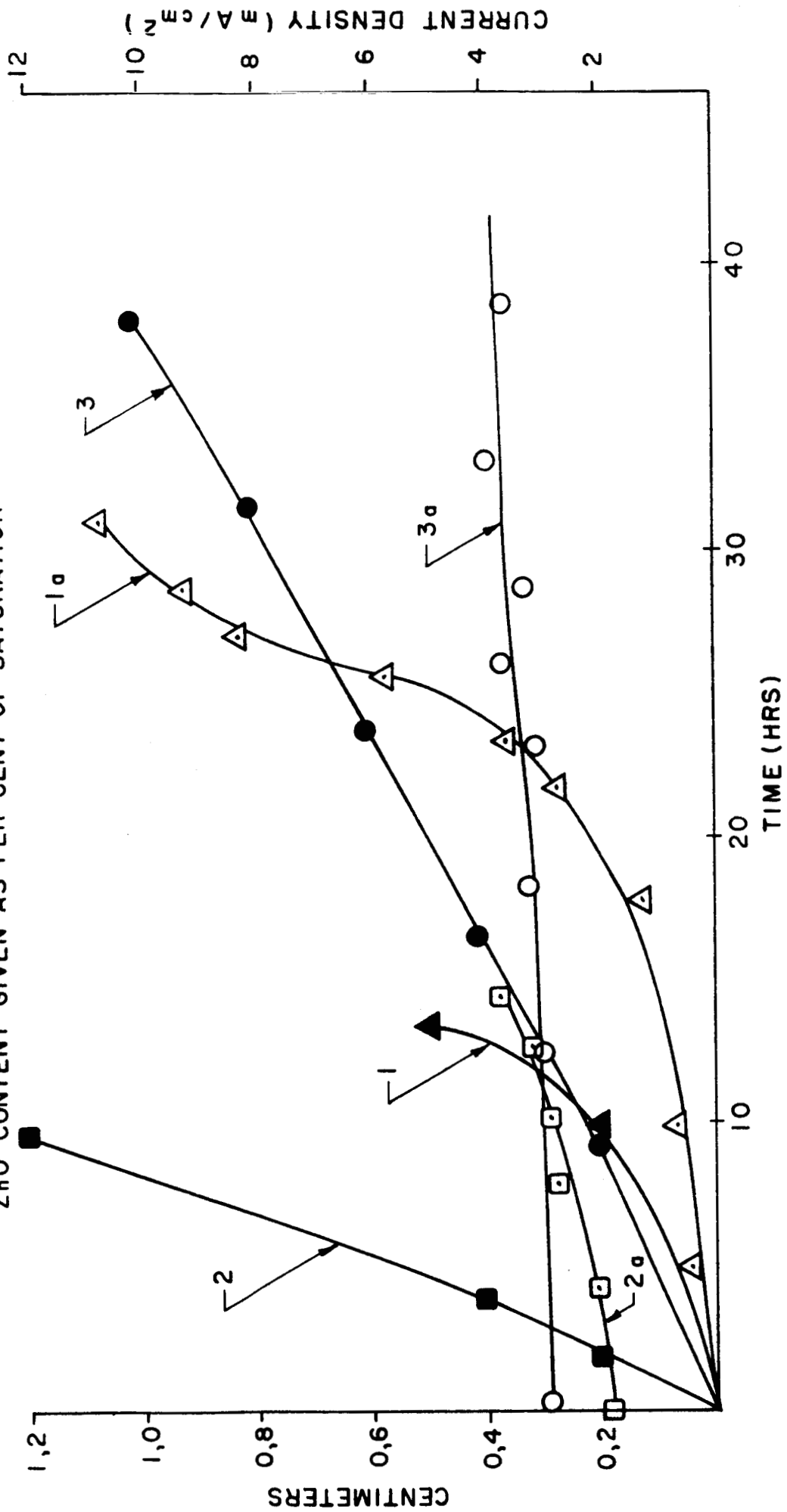


FIG. 21

DEPENDENCE OF THICKNESS OF THE DEPOSIT ON TIME AT VARIOUS ZINC CONCENTRATIONS.

- | | | |
|-------|-----------------|---------------------------------|
| 1a- ○ | CURRENT DENSITY | 144 mV / 44% KOH / 40% SAT. ZnO |
| 1- △ | DISTANCE | |
| 2a- ● | CURRENT DENSITY | 144 mV / 44% KOH / 20% SAT. ZnO |
| 2- ▲ | DISTANCE | |

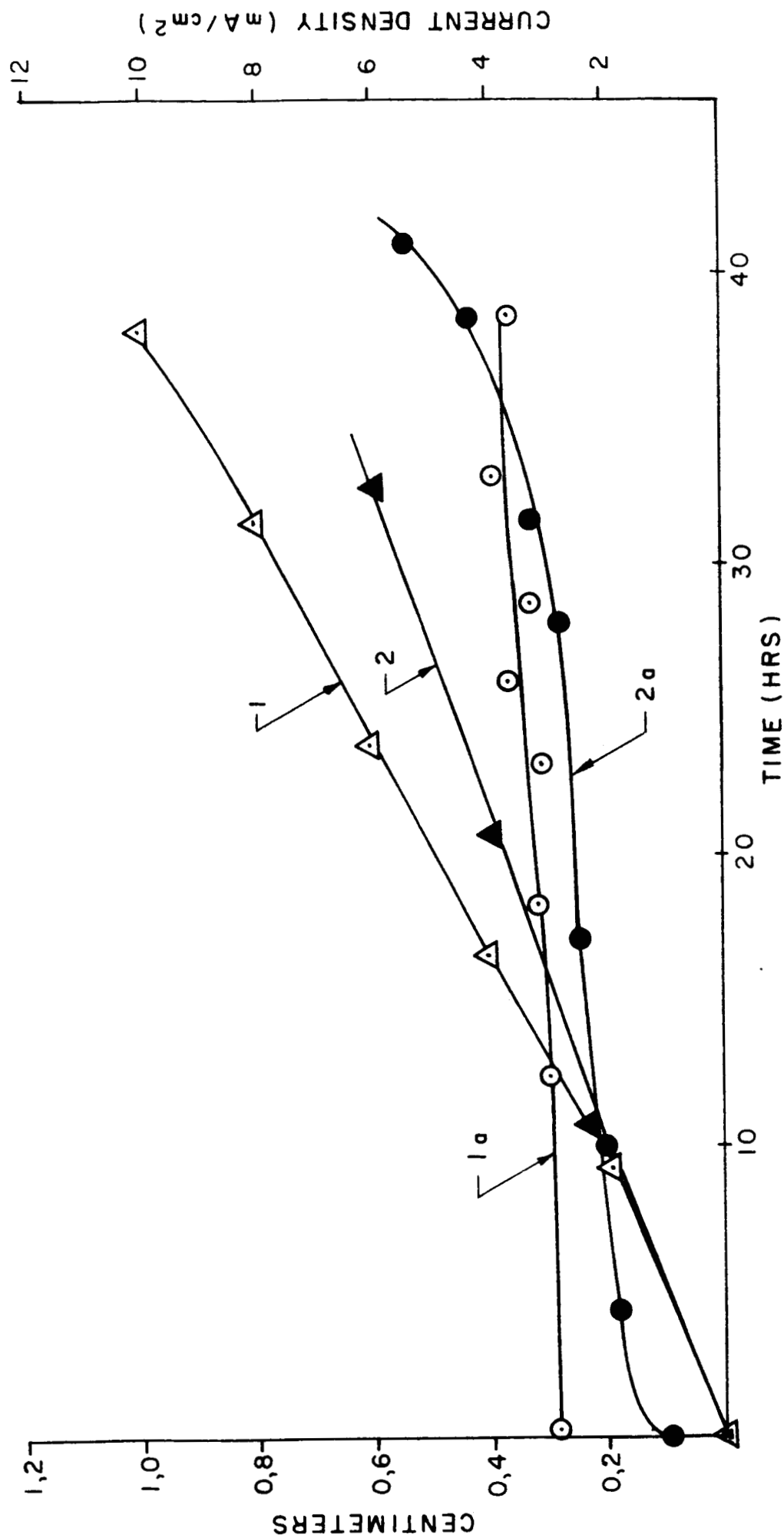


FIG.22

INFLUENCE OF A SURFACTANT ON ZINC DEPOSITION IN THE TUNNEL CELL

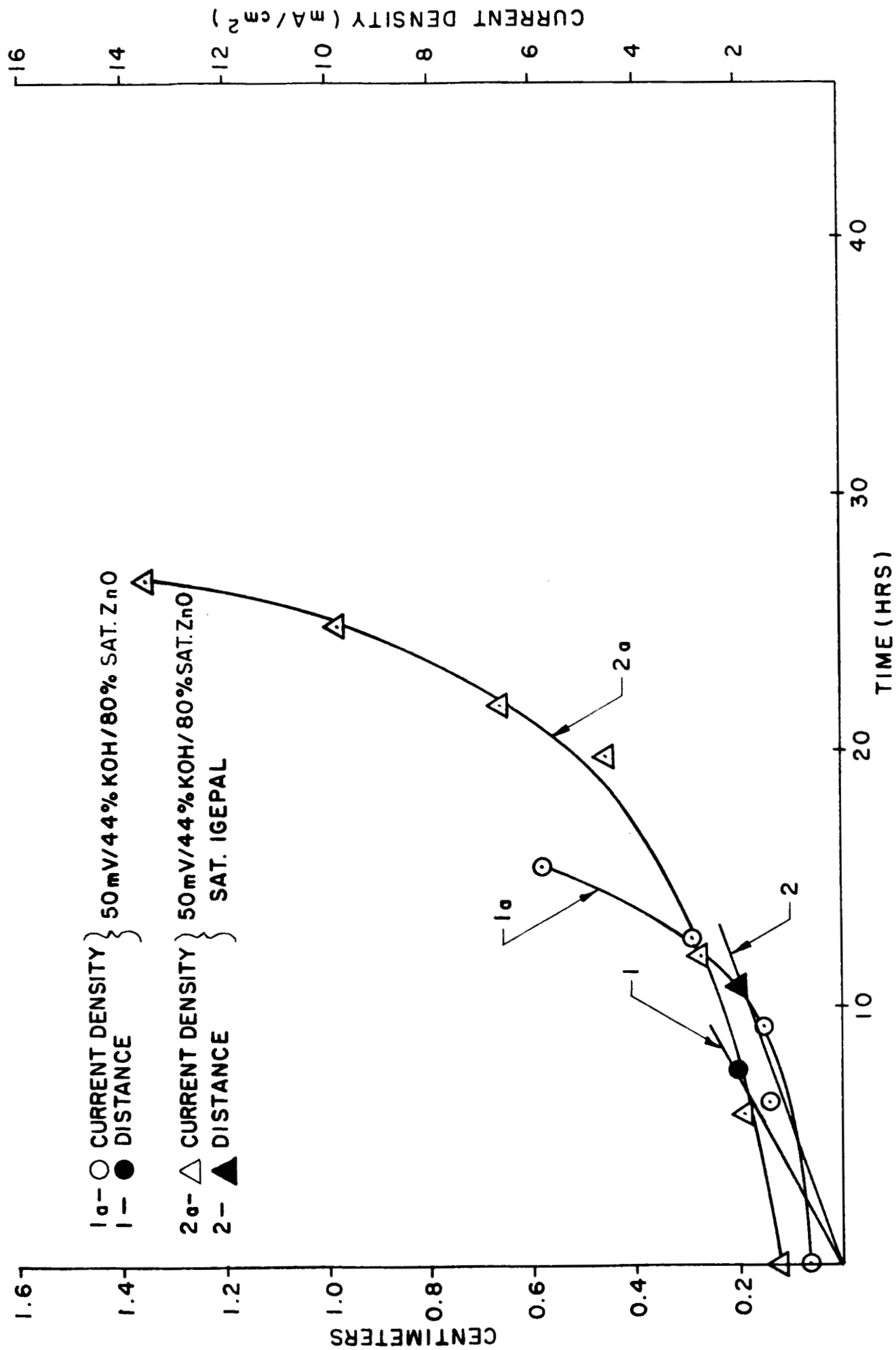


FIG. 23

RATE OF ZINC GROWTH AS A FUNCTION OF TIME.

- 1- ○ 144 mV / 44 % KOH / 20 % SAT. ZnO
- 1a- △ 144 mV / 44 % KOH / 40 % SAT. ZnO
- 2- □ 50 mV / 44 % KOH / 80 % SAT. ZnO
- 2a- ● 50 mV / 44 % KOH / 80 % SAT. ZnO / SAT. IGEPAL
- 3- ▲ 61 mV / 44 % KOH / 40 % SAT. ZnO
- 4- ■ 42 mV / 44 % KOH / 20 % SAT. ZnO

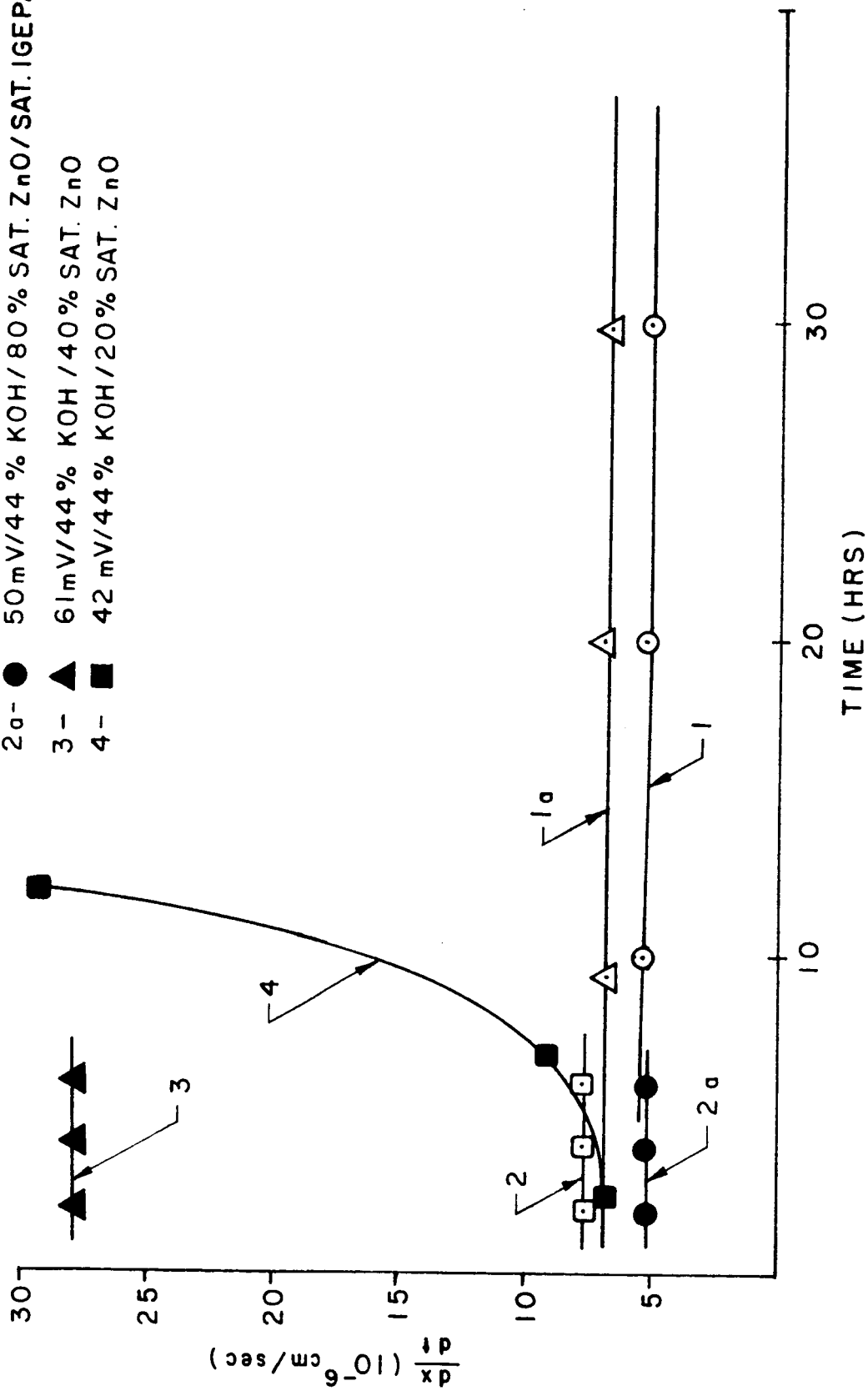


FIG. 24

- 1 - ○ 144 m V/44% KOH/20% SAT. ZnO
- 1a - △ 144 m V/44% KOH/40% SAT. ZnO
- 2 - □ 50 m V/44% KOH/80% SAT. ZnO
- 2a - ● 50 m V/40% KOH/80% SAT. ZnO/IGEPAL
- 3 - ▲ 61 m V/44% KOH/40% SAT. ZnO
- 4 - ■ 42 m V/44% KOH/40% SAT. ZnO

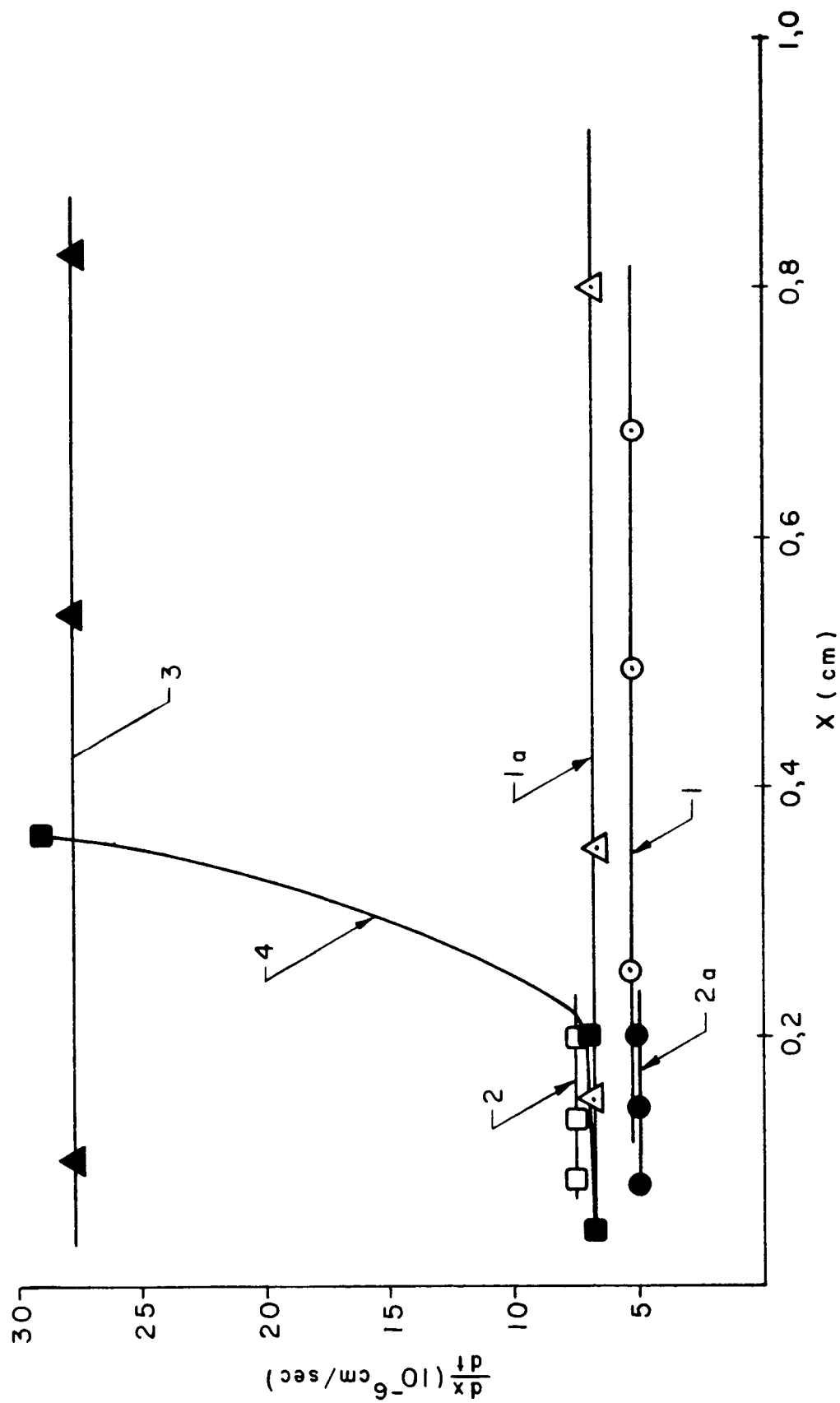


FIG. 25

DENSITY OF ZINC DEPOSITS AS A FUNCTION OF TIME

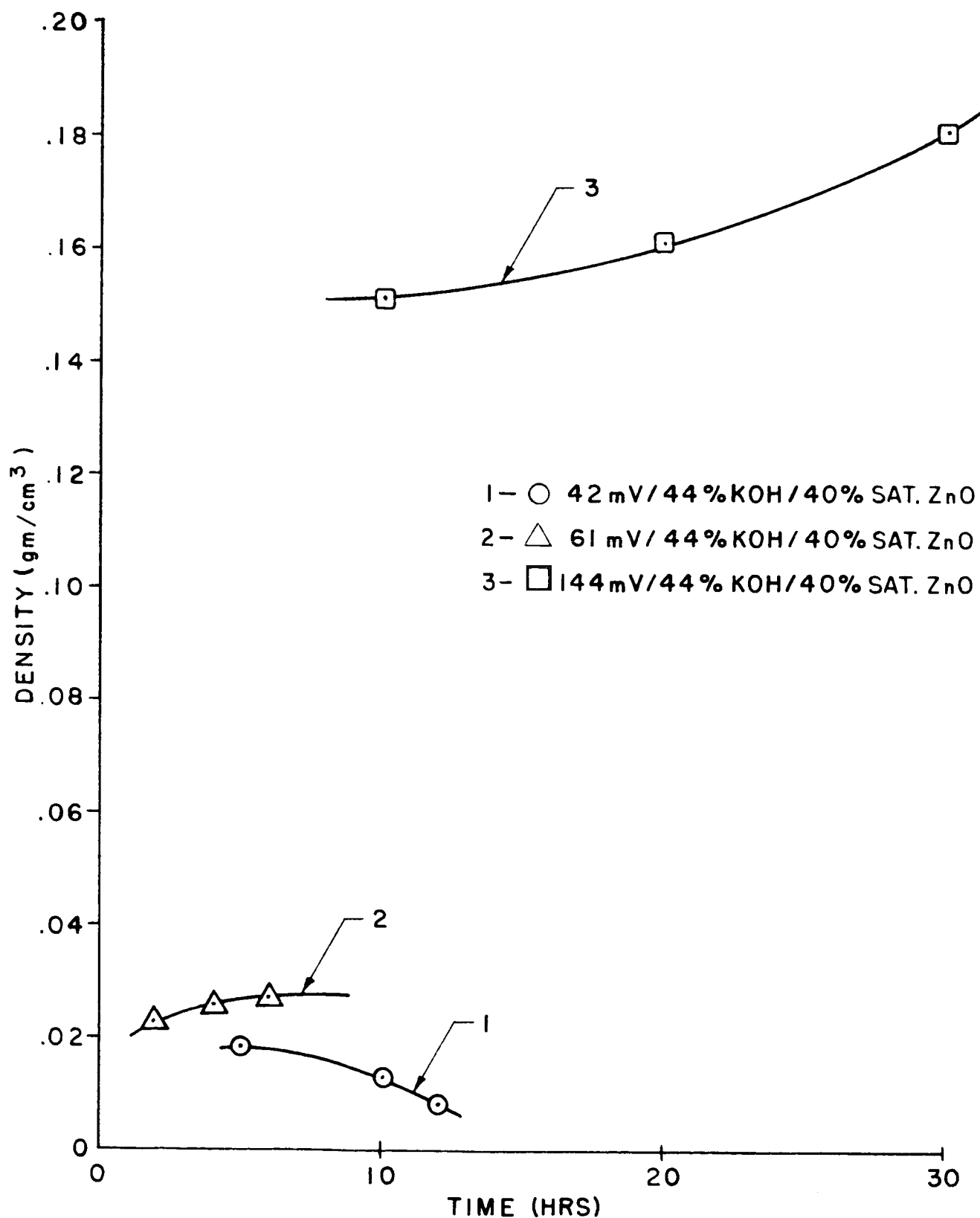


FIG. 26

DENSITY OF ZINC DEPOSIT IN A TUNNEL CELL
AS A FUNCTION OF PLATING OVERPOTENTIAL.

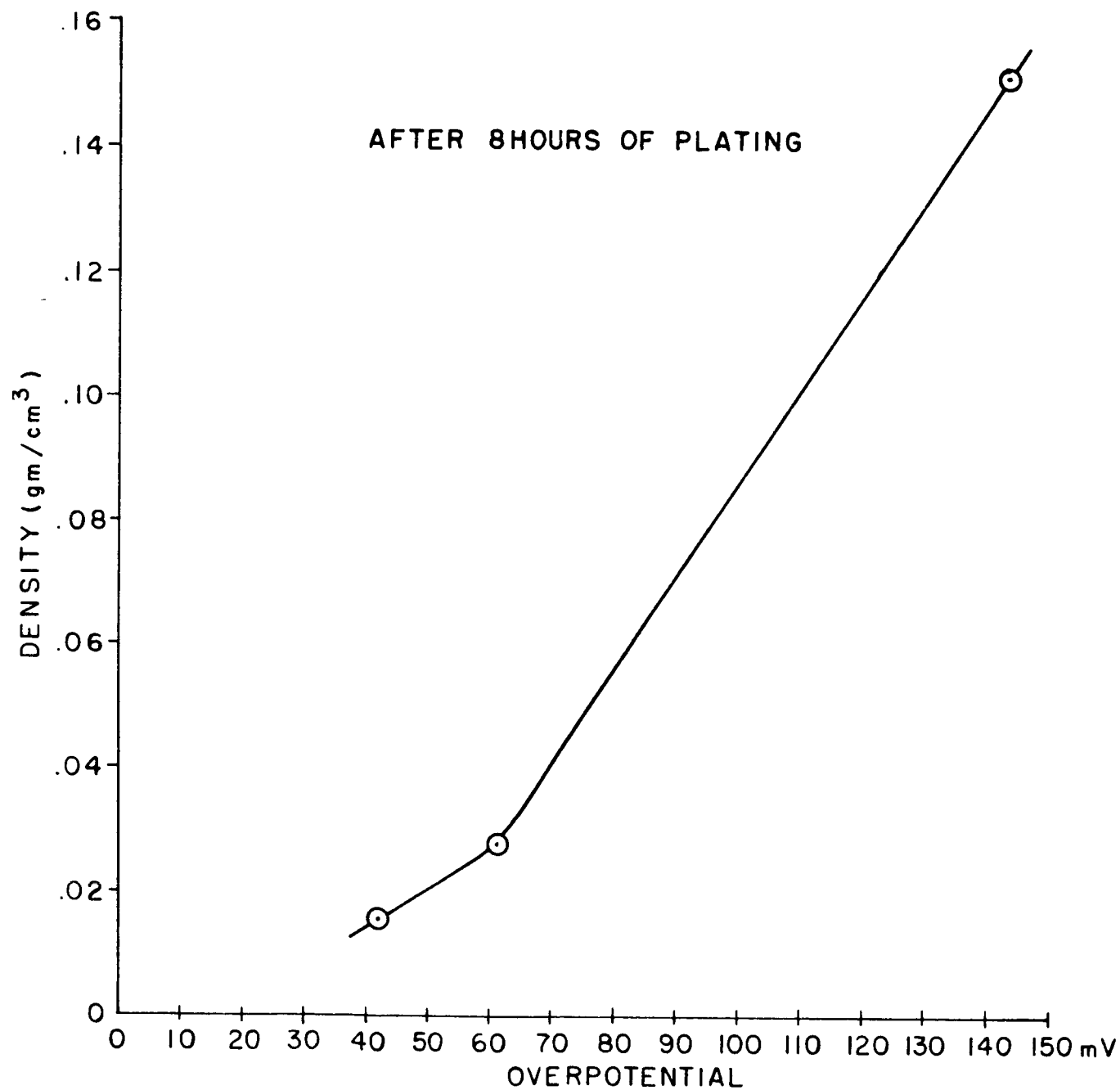


FIG. 27

DENSITY OF ZINC DEPOSITS IN A TUNNEL CELL

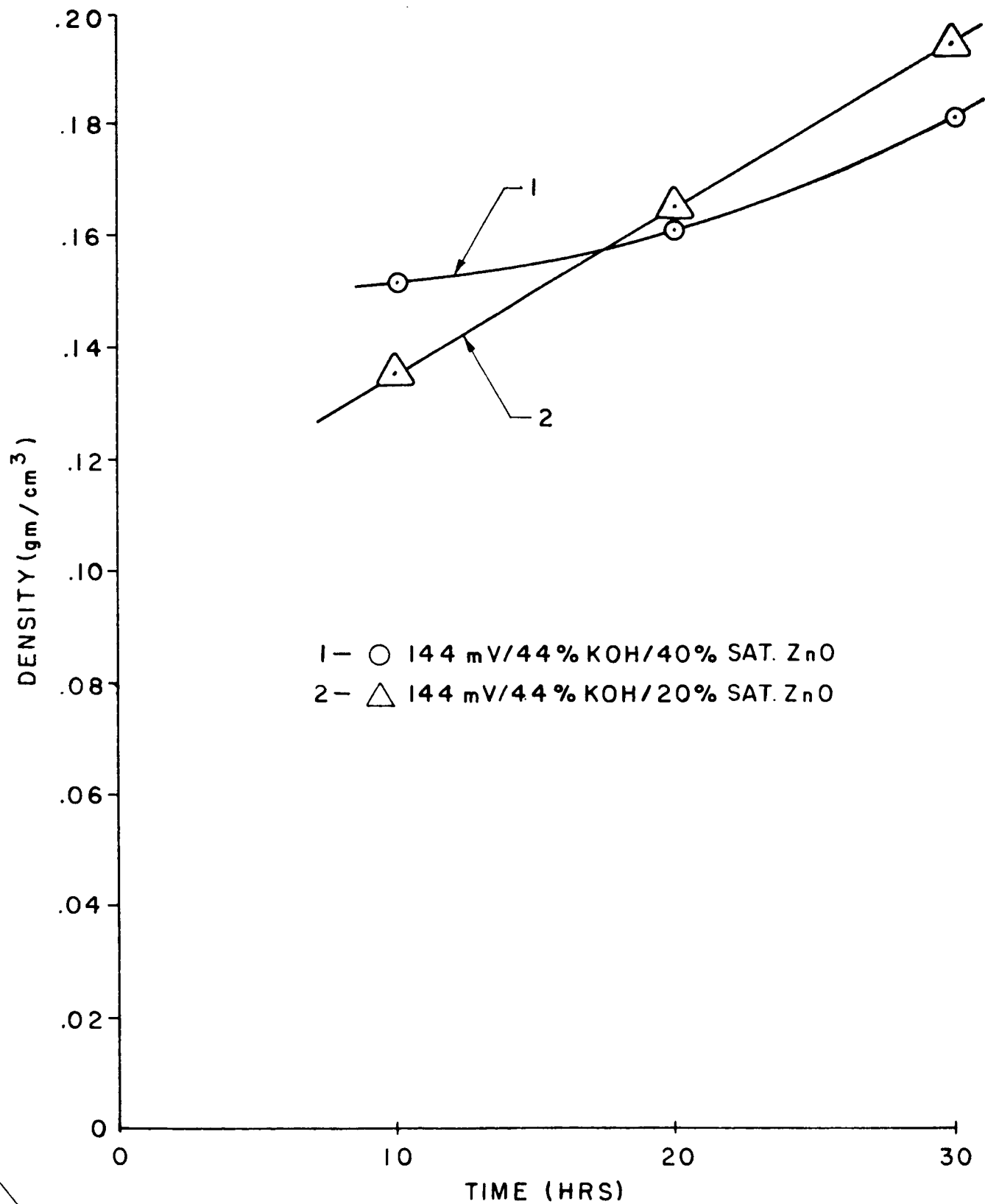


FIG. 28

INFLUENCE OF SURFACTANT ON THE DENSITY OF ZINC DEPOSIT

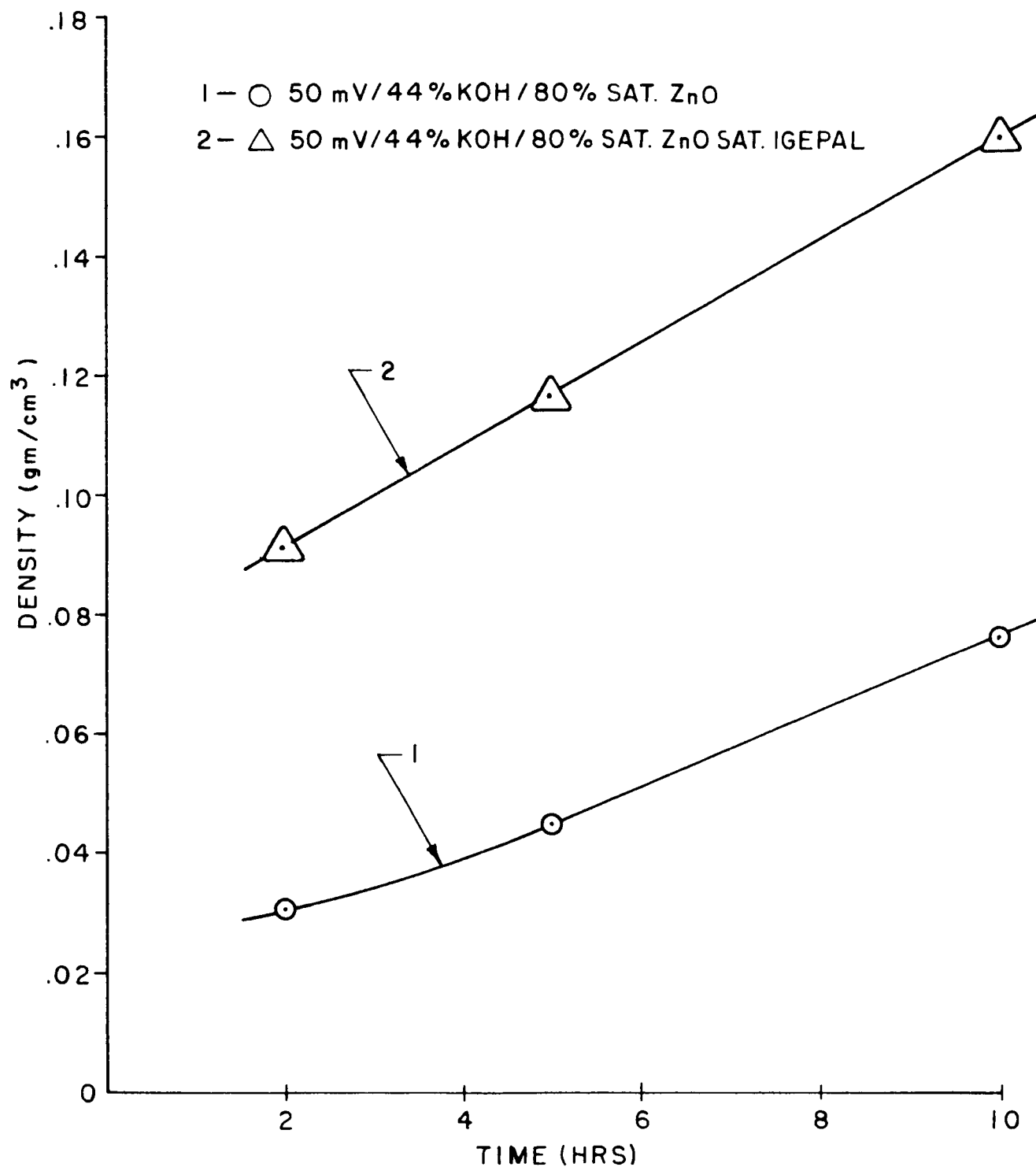
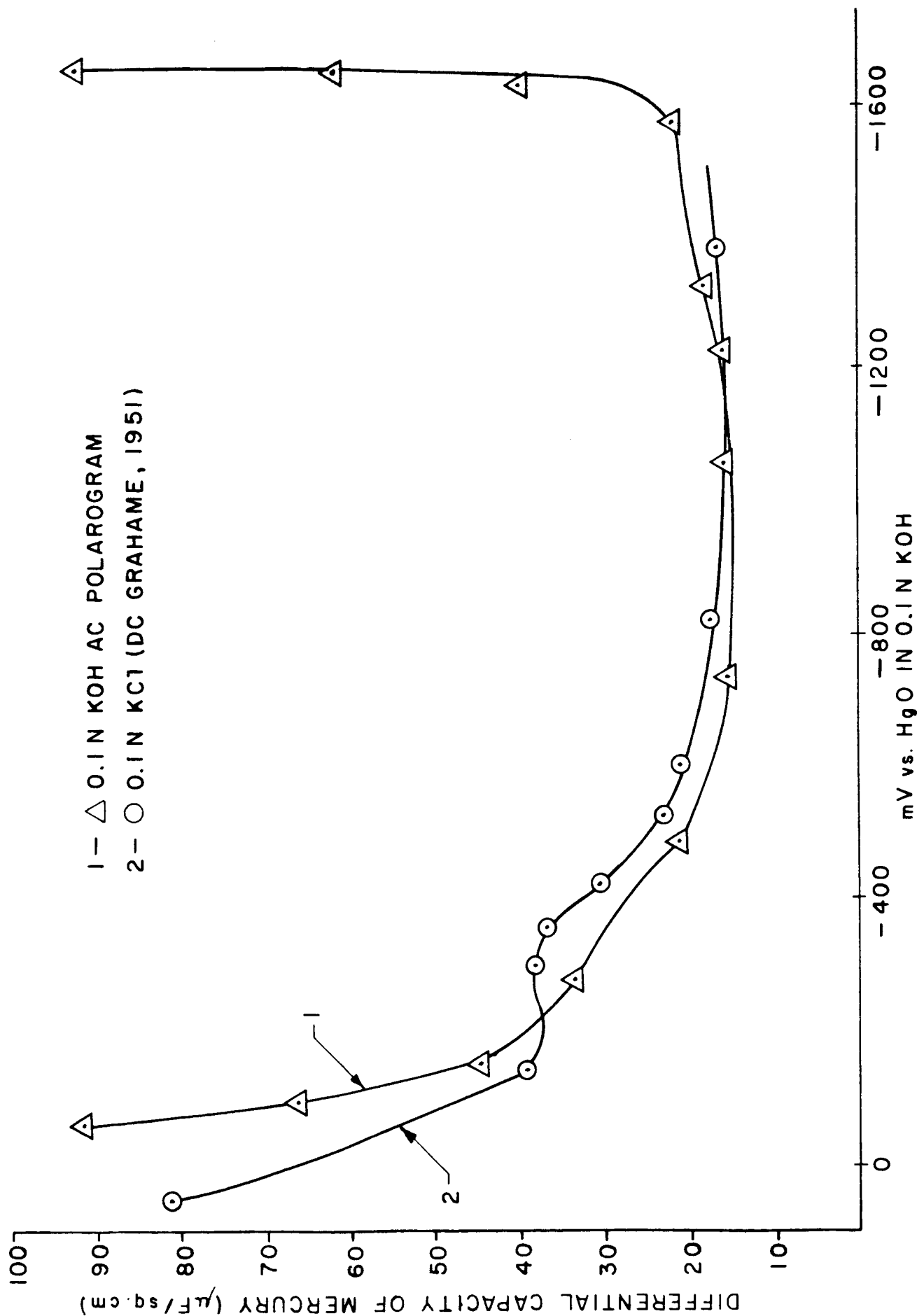


FIG. 29

DOUBLE LAYER CAPACITY OF THE MERCURY DROPPING ELECTRODE



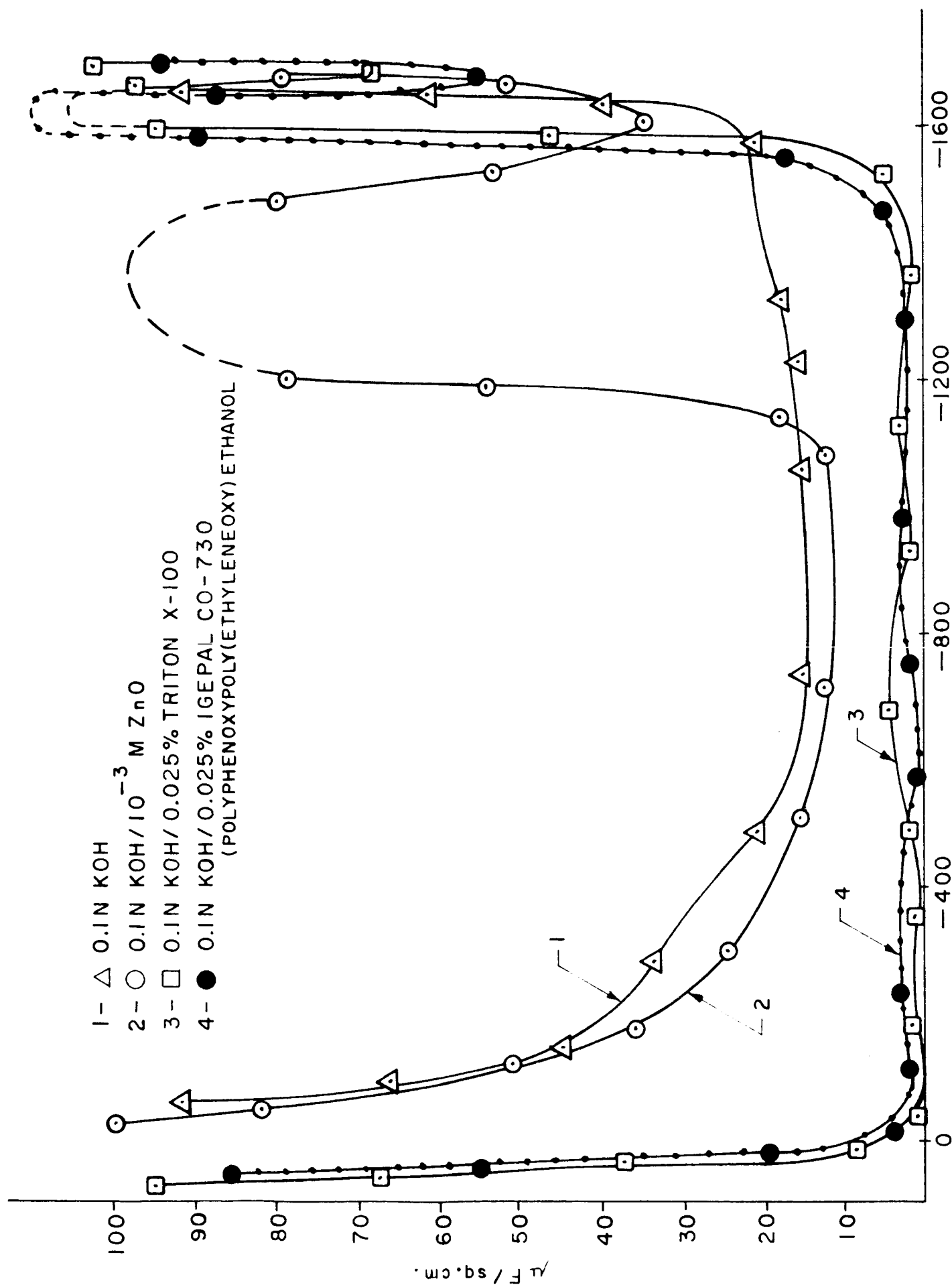


FIG. 31

EFFECT OF SURFACTANTS ON DOUBLE LAYER CAPACITY.

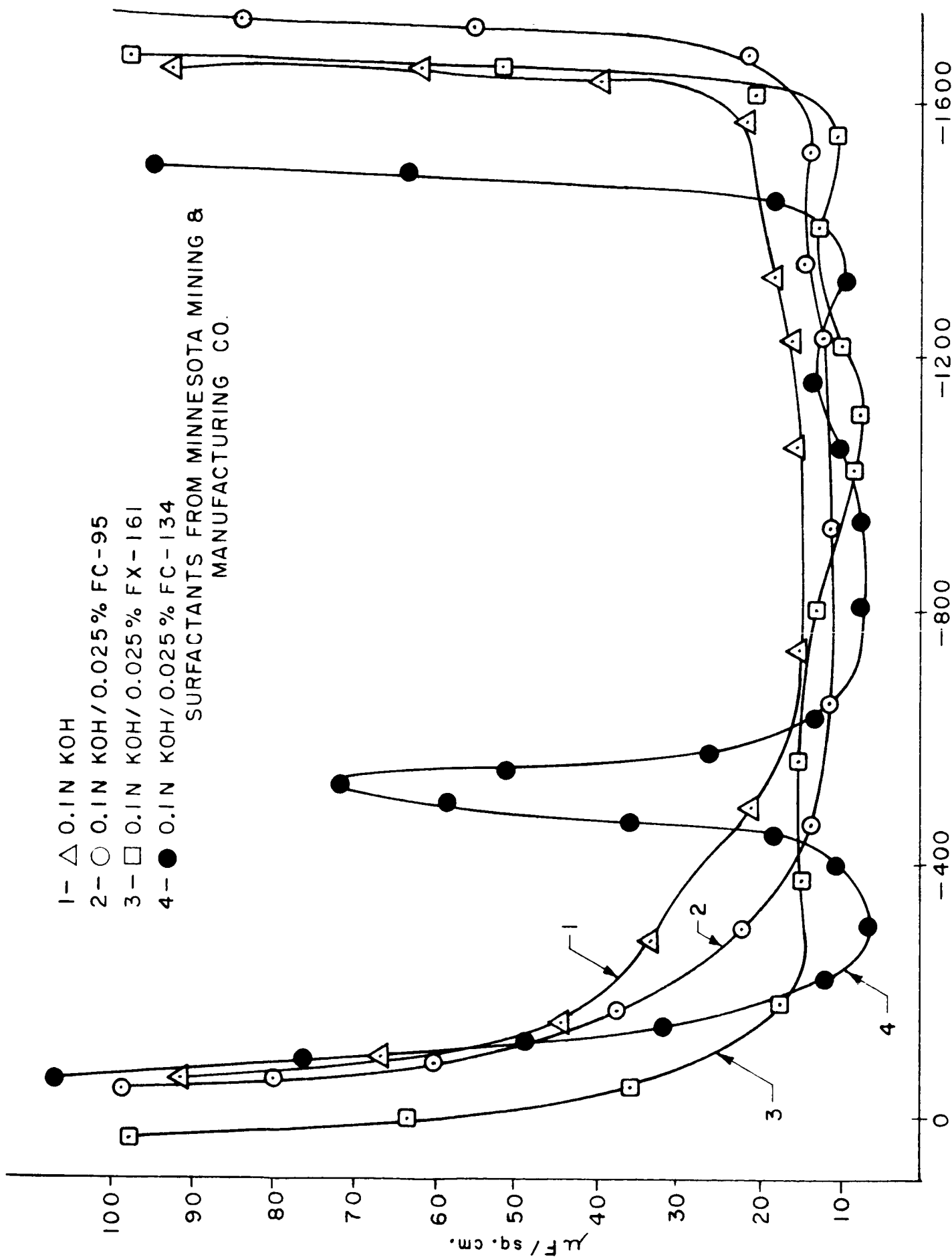


FIG.32

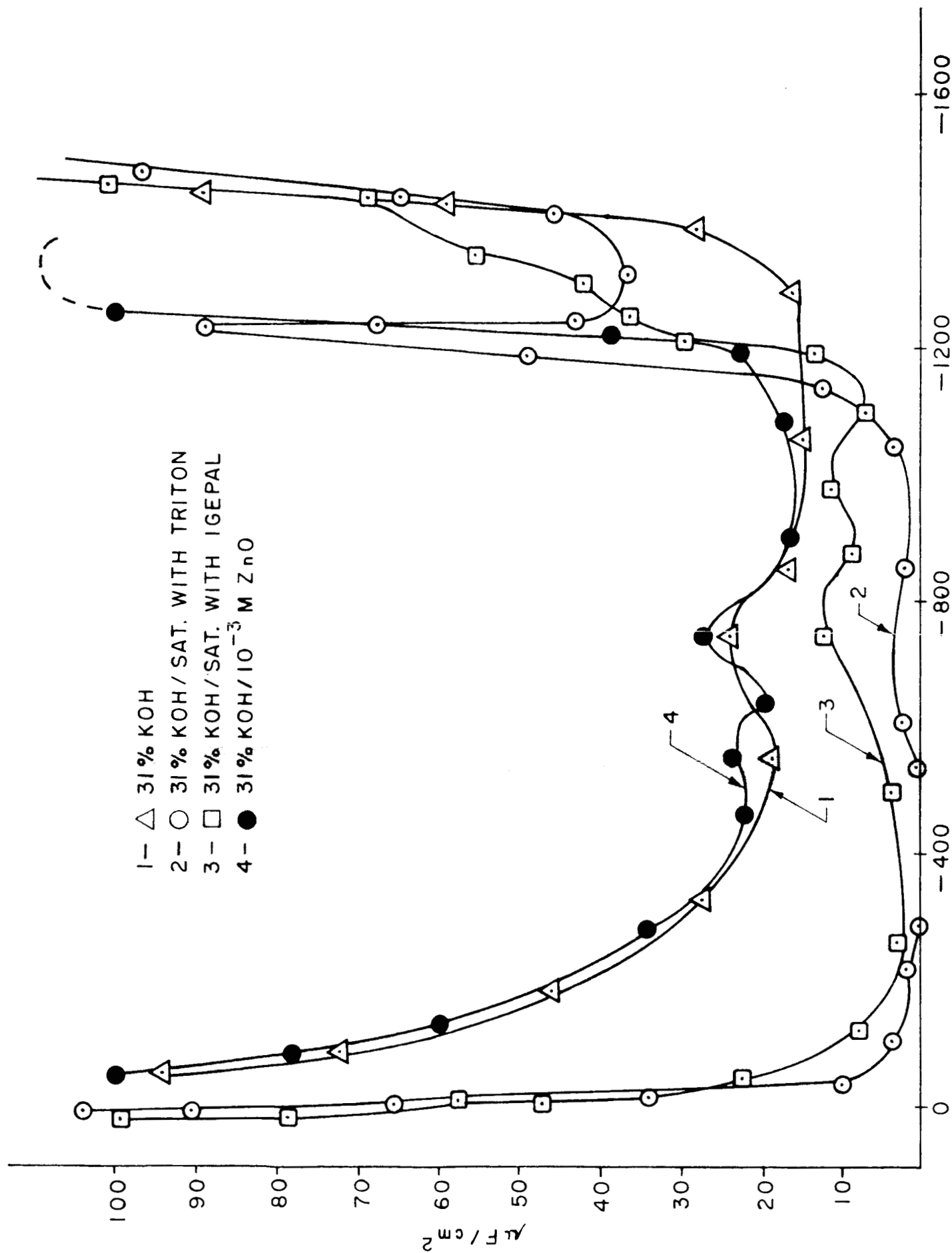


FIG. 33

ZINCATE ADSORPTION ISOTHERMS

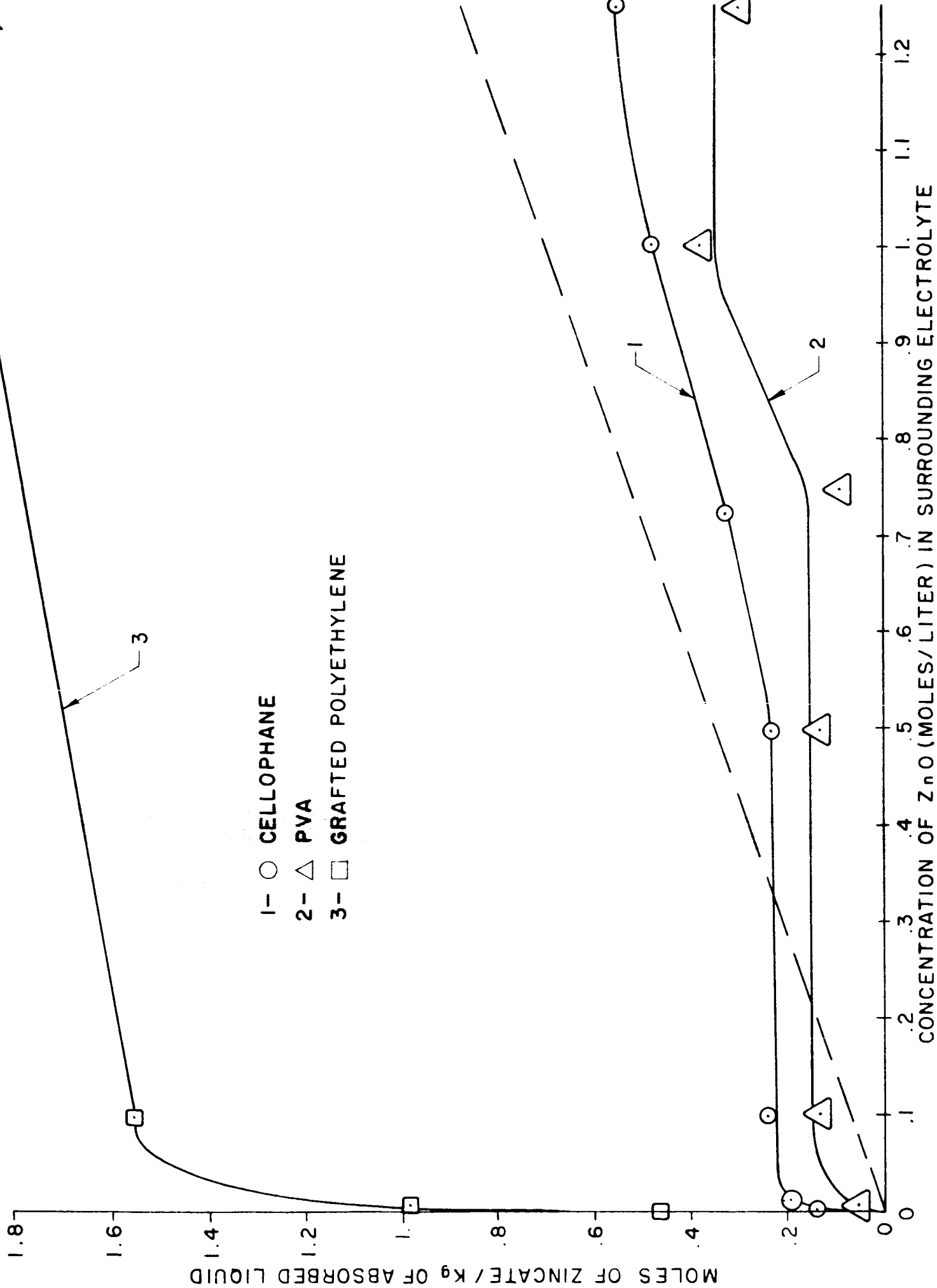


FIG. 34

ADSORPTION ISOTHERMS FOR ZnO IN SEPARATOR

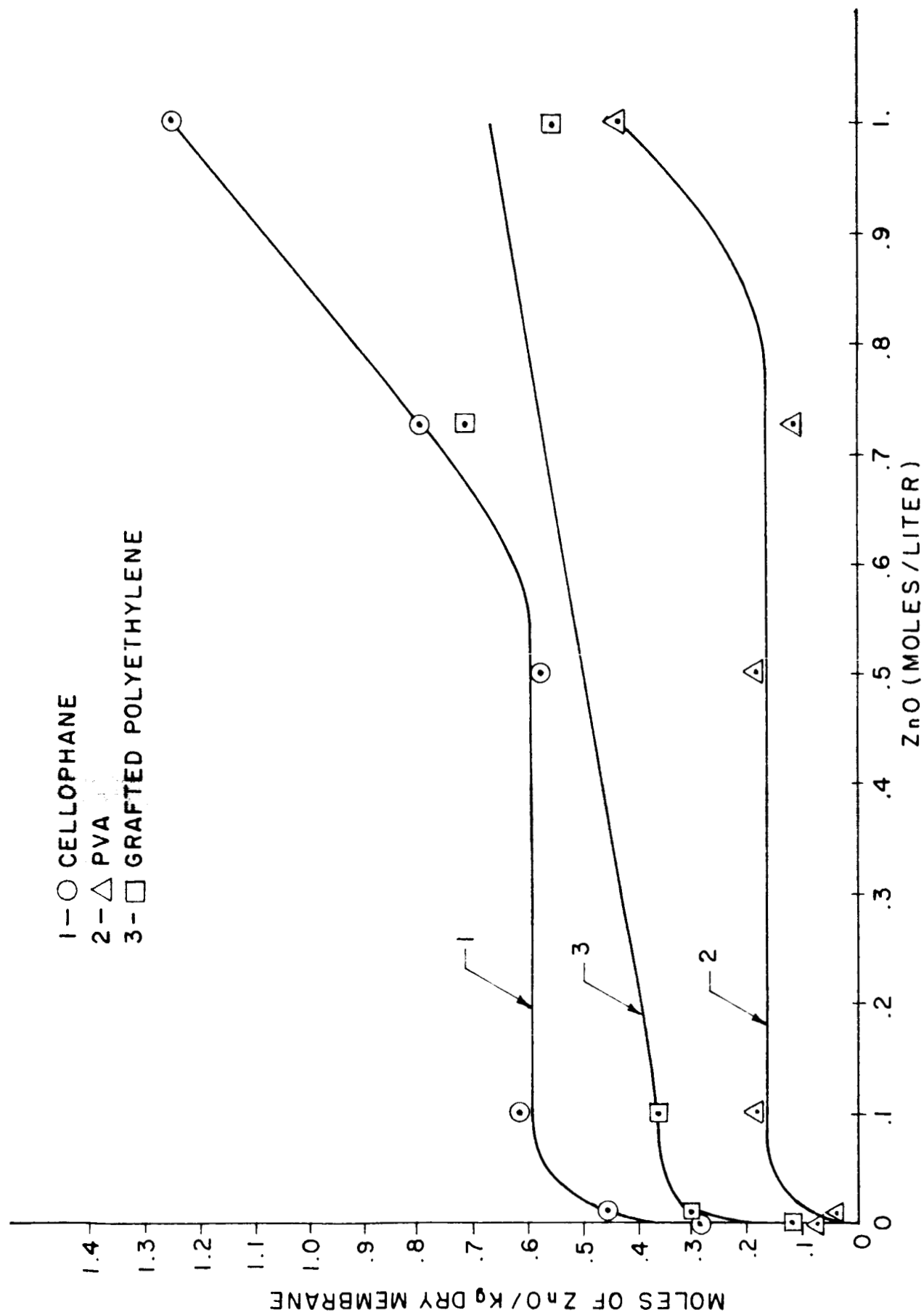


FIG. 35